A COMPUTATIONAL MODEL FOR DETERMININGTHE EFFECTIVE THERMAL CONDUCTIVITY OF A POROUS MEDIUM

By

Daniel K. Lucas

A THESIS

Submitted to
Michigan State University
in partial fulfillment of the requirements
for the degree of

Master of Science

Department of Mechanical Engineering

1996

ABSTRACT

A COMPUTATIONAL MODEL FOR
DETERMINING THE EFFECTIVE
THERMAL CONDUCTIVITY OF
POROUS MEDIUM

By

Daniel K. Lucas

There are many systems of interest in engineering that involve heat transfer through a medium consisting of two or more distinct materials. Such a medium is often considered to be a porous medium when one of the materials is in solid phase and another material is in fluid phase. Some examples of a porous medium are the packed bed of a cooling tower, building insulation, and the core of a catalytic converter. In evaluating these systems and others of interest in engineering thermodynamics, heat transfer, or fluid mechanics, the effective thermal conductivity of a porous medium must first be evaluated. It is difficult to predict the thermal conductivity of a medium consisting of two or more separate materials.

There is no general model to predict the effective thermal conductivity of a porous medium. This paper proposes such a model starting with the two dimensional heat conduction equation. Finite differencing is employed to develop the numerical model. From this numerical model, a computer code is developed that predicts the effective thermal conductivity of a porous medium.

To my wife and family: Susan, Lisa, Kerri, and Daniel.

TABLE OF CONTENTS

LIST OF FIGURES

Nomenclature

k	Thermal Conductivity
L	Length
q	Heat Transfer Rate
T	Temperature
A	Area
R	Thermal Resistance
d	Diameter
F	Average Temperature Gradient
DT	Time Step

Symbols

ε	Porosity
γ	Solid Thermal Conductivity / Fluid Thermal conductivity
γ	Geometrical Factor
ε	Void Fraction

Subscripts

f	Fluid
l	Lower Boundary
m	Effective Value
u	Upper Boundary
s	Solid
p	Pore
c	Continuous Phase
d	Discontinuous Phase
T	Top Cell Node
B	Bottom Cell Node
R	Right Cell Node
L	Left Cell Node
i	Index Transverse to Heat Flow
j	Index Parallel to Heat Flow

Superscripts

k	Index Direction

Overbar

$\bar{}$	Average Conditions

CHAPTER I

INTRODUCTION

1.1 Problem Statement

There are many systems of interest in engineering that involve heat transfer through a medium consisting of two or more distinct materials. Such a medium is often considered to be a porous medium when one of the materials is in solid phase and the other material is in fluid phase. Some examples of a porous medium are the packed bed of a cooling tower, building insulation, and the core of a catalytic converter. In evaluating these systems and others of interest in engineering thermodynamics, heat transfer, or fluid mechanics, the effective thermal conductivity of a porous medium must first be evaluated. The thermal conductivity of a single material is defined as the amount of heat flowing by conduction through a unit area per unit time per unit temperature gradient. The evaluation of thermal conductivity for a single material is very straight forward. However, it is more difficult to predict the thermal conductivity of a medium consisting of two or more separate materials.

There has been previous work to determine the thermal conductivity of a porous medium. However, this work has dealt with either specific systems or specific geometries, and there is no general model for evaluating the effective thermal conductivity of a two component system.

There are three modes of heat transfer in a porous medium: conduction, convection, and radiation. Conduction is heat transfer by molecular, atomic, and electronic motion, and is often the prominent mode of heat transfer. Convection is heat transfer by fluid motion and can be important as porosity increases. Finally, radiation is heat transfer by electromagnetic wave motion and becomes increasingly important as the temperature increases.

The problem will be studied as a two-dimensional system similar to the system shown in Figure 1. This system consists of two or more anisotropic materials having different thermal characteristics and has fixed temperatures applied to the top and bottom surfaces and adiabatic sidewalls. The effective thermal conductivity is defined as k_m such that the heat transfer may modeled using the equation

$$\bar{q} = \frac{k_m \Delta T}{L}. \qquad (1)$$

Using the above equation, a control volume may be defined, that is small enough to have local thermal equilibrium yet large enough to retain the properties of the porous medium, over which Fourier's law of heat conduction is valid, i.e.,

$$\underset{\sim}{q} = k_m \nabla T. \qquad (2)$$

1.2 Literature Review

Previous work by Baradat and Combarnous [1] has shown that the two simplest models for determining effective thermal conductivity also describe the

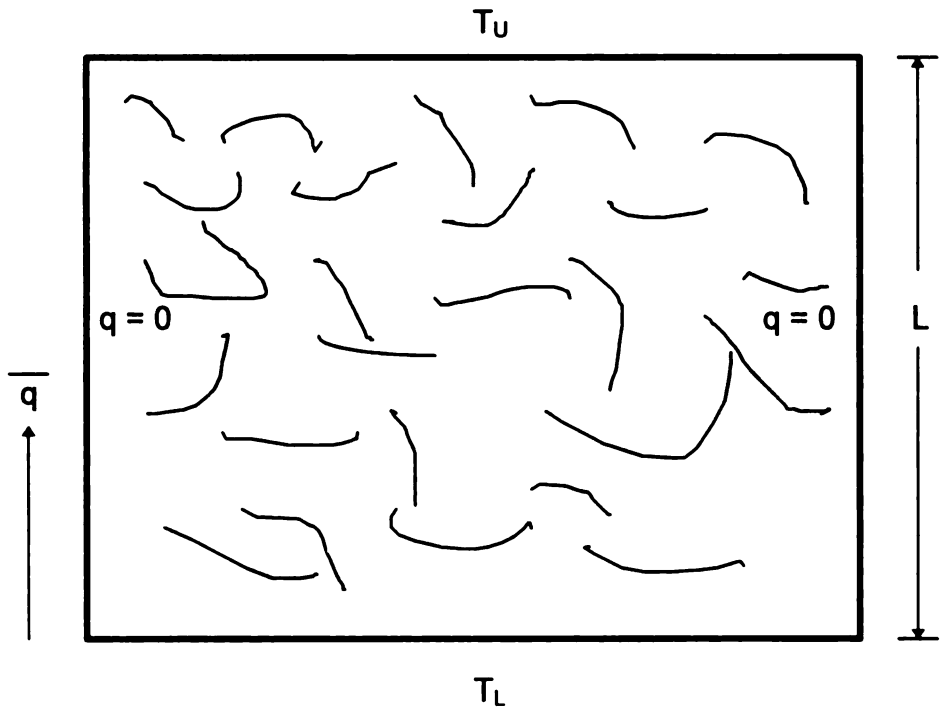

Figure 1. Conductive Heat Transfer in Porous Medium

upper and lower boundaries for the actual thermal conductivity of a porous medium. These are the parallel resistance model and the series model. In the parallel resistance model, the voids and solids hypothetically move in opposite directions transverse to the heat flow as shown in Figure 2. Working with the parallel thermal circuit shown in Figure 3, the thermal conductivity can be shown to be

$$\frac{k_m}{k_f} = \varepsilon + (1 - \varepsilon)\gamma \tag{3}$$

where ε is the porosity and γ is the ratio of solid thermal conductivity to the fluid thermal conductivity. In the series resistance, the voids and solids hypothetically move in opposite directions in the direction of the heat flow as in Figure 4. Now, working with the series thermal circuit shown in Figure 5, the thermal conductivity can be shown to be

$$\frac{k_m}{k_f} = \left[\varepsilon + \frac{(1 - \varepsilon)}{\gamma}\right]^{-1}. \tag{4}$$

The current models are bounded by the series and parallel models as shown in the graph in Figure 6 as k_m/k_f versus porosity with the solid to fluid thermal conductivity ratio, γ, set equal to 0.1.

These two simple models represent a whole group of models that have simple solutions. In these simple models, either heat flow lines run parallel to the direction of the heat flux or the isotherms are perpendicular to the heat flow. The group of models based on these simple models have one common approach for solution. They use a thermal circuit network and allow the

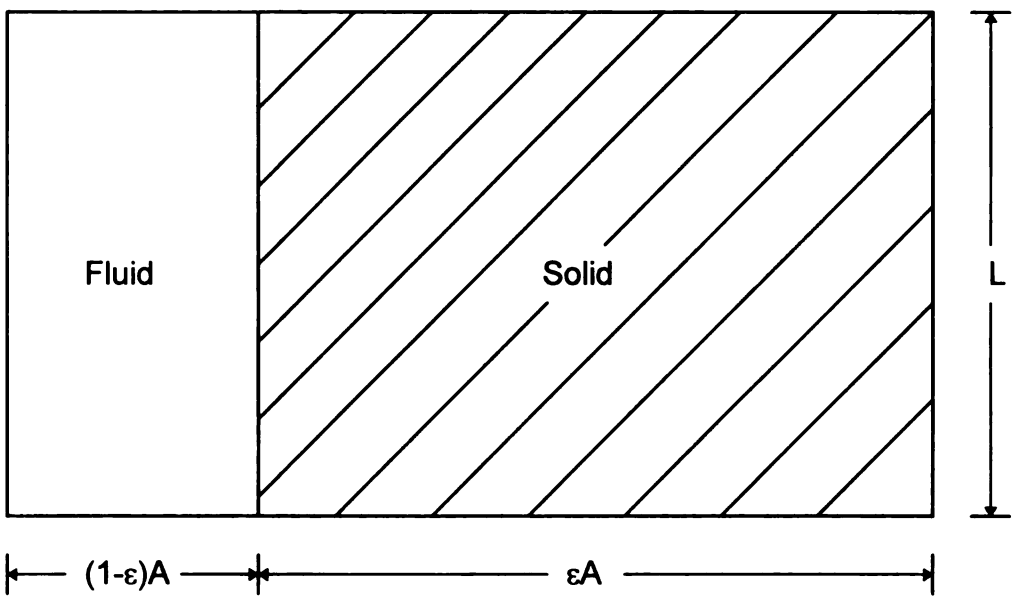

Figure 2. Parallel Resistance Model

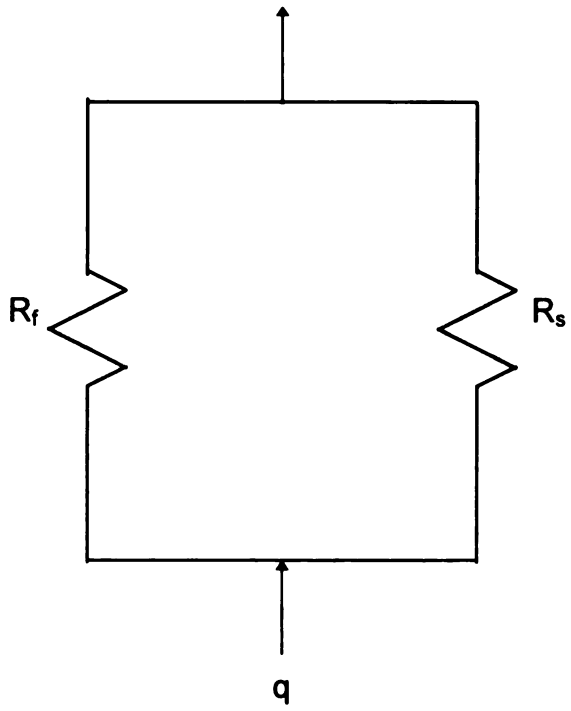

Figure 3. Parallel Resistance Circuit

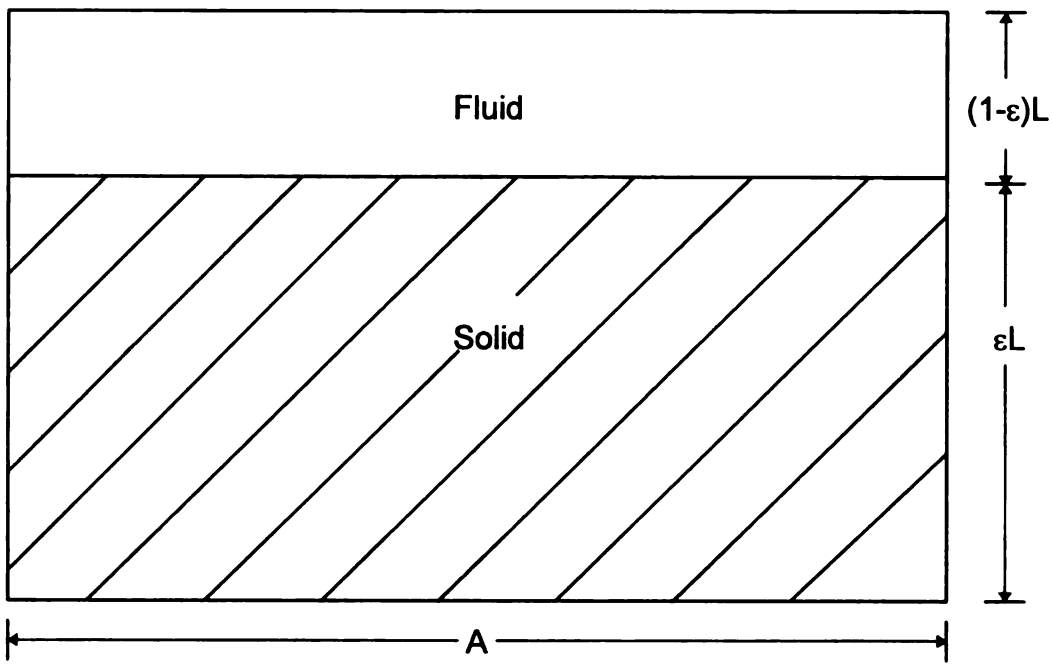

Figure 4. Series Resistance Model

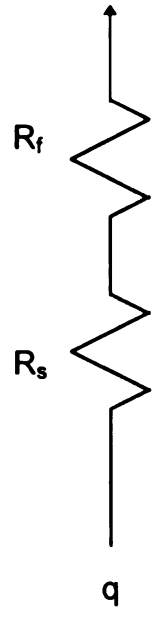

Figure 5. Series Resistance Circuit

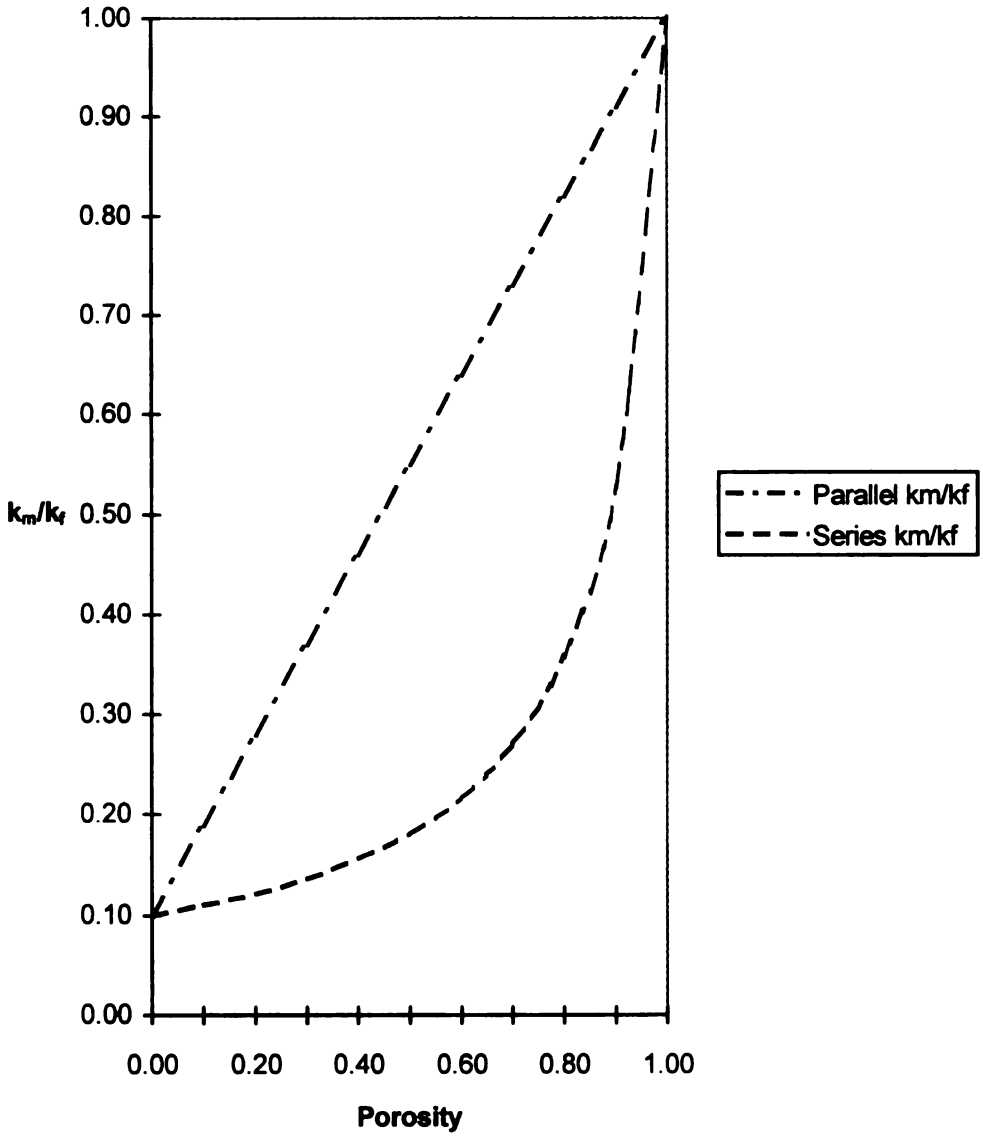

Figure 6. Parallel and Series Models of Effective Thermal Conductivity for $\gamma = 0.1$

problems to be solved by means of reducing them to algebra and geometry.

Numerous models have been proposed to make use of the simple solutions. Russell [2] proposes that porous media be modeled as cubical pores in a cubic lattice arrangement and developed

$$\frac{k_m}{k_f} = (1 - \varepsilon)^{1/3}\gamma + \left(\frac{\varepsilon}{\varepsilon^{2/3} + (1 - \varepsilon)^{2/3}\gamma}\right)^{-1}. \qquad (5)$$

Another model proposed by Loeb [3] views the porous medium as a square matrix with a lattice of pores situated inside the matrix. The effective thermal conductivity as determined by Loeb is

$$\frac{k_m}{k_f} = (1 - \varepsilon_1) + \frac{\varepsilon_1}{\frac{\varepsilon_2 k_s}{k_p} + (1 - \varepsilon_2)} \qquad (6)$$

where ε_1: perpendicular void fraction

ε_2: parallel void fraction

k_p: $4\gamma d e \sigma T^3$

and γ: geometrical factor

d: largest dimension of pore in direction of heat flow.

Figure 7 shows Loeb's model and the corresponding thermal circuit is shown in Figure 8. Note that the effective thermal conductivity, k_p, of a pore is a function of radiative heat transfer. This is a disadvantage when the fluid is a liquid rather than a gas due to the opaque nature of most liquids. Woodside [4] modeled a porous medium putting a matrix of spheres in a continuum. Using this model, he

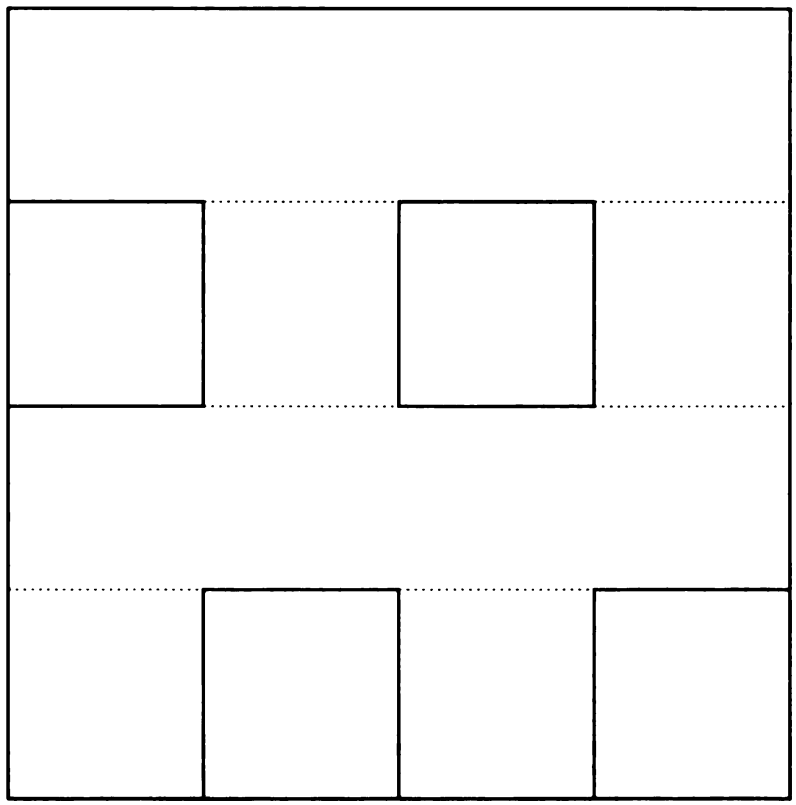

Figure 7. Loeb's Model

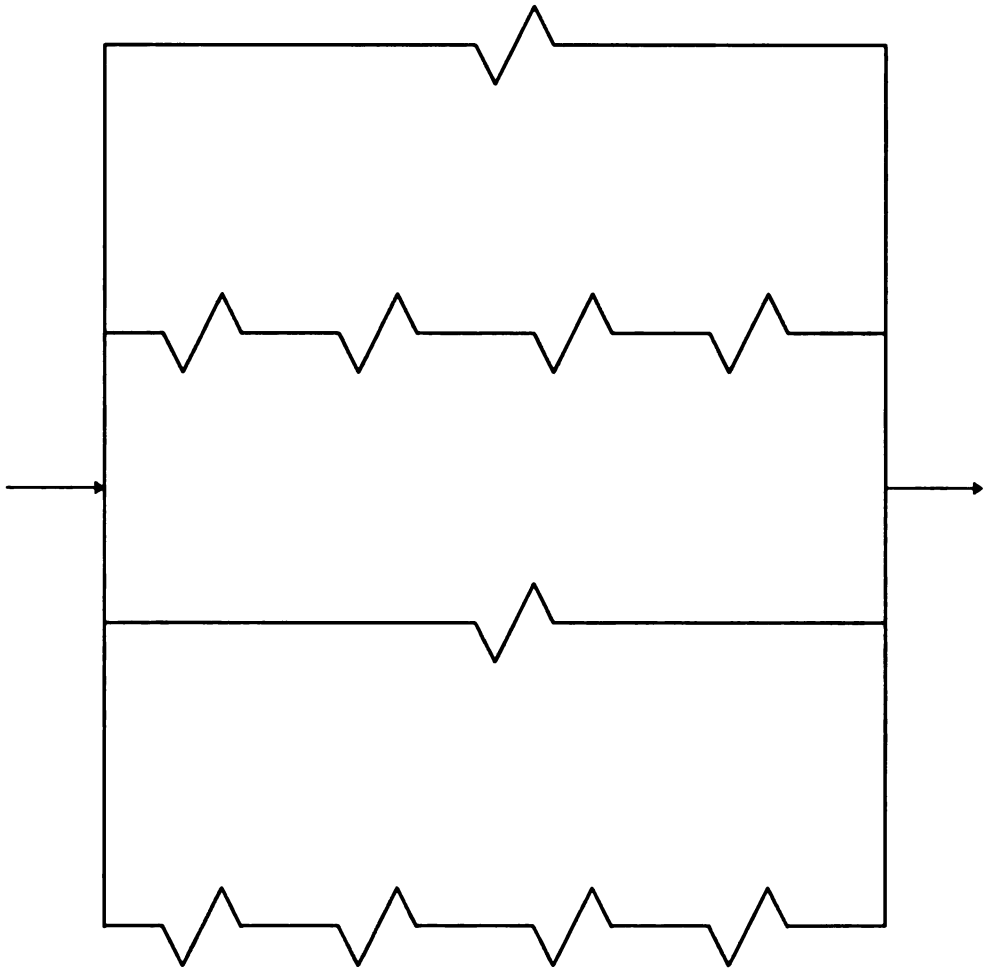

Figure 8. Thermal Circuit of Loeb's Model

determined the equation for the effective thermal conductivity of a porous medium to be

$$\frac{k_m}{k_c} = \left\{1 - \left(\frac{d\varepsilon_d}{\pi}\right)^{1/3}\left[1 - \frac{a^2-1}{a}\ln\left(\frac{a+1}{a-1}\right)\right]\right\}^{-1} \tag{7}$$

where

$$a = \left[1 + \frac{4}{\pi\left(\frac{k_d}{k_c} - 1\right)\left(\frac{6\varepsilon_d}{\pi}\right)^{2/3}}\right]^{1/4} \tag{8}$$

and c and d denote the continuous and discontinuous phase respectively. This relation is valid only where

$$0 \le e_d \le 0.5236 .$$

There are many geometries that can be used to develop expressions for the effective thermal conductivity of a porous medium. Specifying a geometry and developing the corresponding thermal circuit can, in principle, be reasonably straight forward. However, the geometry and algebra may make obtaining an expression for the effective thermal conductivity very difficult. Other geometries have been investigated by Godbee and Ziegler [5], Luikov, et. al. [6] and Krupicka [7] and corresponding expressions for effective thermal conductivity of these porous media have been developed.

The exact solution of Laplace's equation forms the basis for another group of models. Many of these are heat transfer applications that have been developed from electromagnetic applications. Using a heterogeneous body

composed of an element with one thermal conductivity value inserted into another larger element having another thermal conductivity, Maxwell [8] developed an expression for the effective thermal conductivity

$$k_m = k_c\left[\frac{k_d + 2k_c - 2\varepsilon_d(k_c - k_d)}{k_d + 2k_c + \varepsilon_d(k_c - k_d)}\right] . \tag{9}$$

This solution is based on an explicit assumption that the spheres have no influence on one another due to the distance between. Therefore, it is implicit that the expression above is good only as the porosity, ε_d gets small. To account for influence between spheres, Rayleigh [9] developed models for spheres in a cubic array and cylinders in a square array. He obtained the equation

$$\frac{k_m}{k_f} = \frac{\dfrac{\left(2 + \dfrac{k_d}{k_c}\right)}{\left(1 - \dfrac{k_k}{k_c}\right)} - 2\varepsilon_d}{\left(\dfrac{2 + \dfrac{k_d}{k_c}}{1 - \dfrac{k_d}{k_c}}\right) + \varepsilon_d} \tag{10}$$

for the cylindrical model.

More general solutions were developed by assuming the particles to be ellipsoids. Fricke [10] developed the expression

$$k_m = k_c\left[\frac{1 + \varepsilon_d\left(F\dfrac{k_d}{k_c} - 1\right)}{1 + \varepsilon_d(F - 1)}\right] \tag{11}$$

where

$$F = \frac{1}{3}\sum_{i=1}^{3}\left[1 + \left(\frac{k_d}{k_c} - 1\right)f_i\right]^{-1} \tag{12}$$

and

$$\sum_{i=1}^{3} f_i = 1. \tag{13}$$

The ratio of the overall average temperature gradients in the solid and the fluid phases is represented F and the semi-principle axes of the ellipsoid are represented by f_i. As with Maxwell, Fricke also assumed no particle to particle interactions in his model.

Laplace's equation is solved over one fourth of a cell for spheres in a cubic array and cylinders in a square array by Krupiczka [7]. A nearly unusable and very complex mathematical expression is obtained for the effective thermal conductivity by applying artificial boundary conditions.

The solution for a matrix of particles that are in or are nearly in contact with one another is obtained by Batchelor and O'Brien [11]. They developed this solution for systems where γ is large. They developed the expression

$$\frac{k_m}{k_f} = 4.01 \ln\gamma \tag{14}$$

for the special case where a random array of uniform spherical particles are in contact with one another.

There are some empirical and numerical models being used to determine the effective thermal conductivity of a porous medium. Numerical models may

also be used to obtain simplified solutions to the series resistance and the parallel resistance models. Woodside and Messmer [12] noted that the distribution for the parallel model corresponds to a weighted arithmetic mean and the distribution for the series model corresponds to a weighted harmonic mean. An intermediate model has been proposed by developing the weighted geometric mean which is expressed by

$$\frac{k_m}{k_f} = \varepsilon \frac{k_s}{k_f}. \tag{15}$$

This expression is the foundation for the most widely used empirical relationship,

$$\frac{k_m}{k_f} = C\varepsilon \frac{k_s}{k}. \tag{16}$$

This expression was first proposed and obtained empirically by Lichtender [13]. C is an empirical constant that is adjusted to fit the experimental data. Yet another proposed relationship is

$$k_m = k_s(1 - \varepsilon). \tag{17}$$

This expression was proposed by Francl and Kingery [14] who conducted experiments on a test section with a fabricated porosity of isometric spherical pores and anisometric cylindrical pores using air as the fluid. They were able to correlate their data for temperatures below 500°C. There have been other empirical expressions developed, however, they are of limited in usefulness.

Another numerical model is developed by Jaguaribe and Beasley [15]. In this model, they consider radial flow in a porous medium as an array of solid

cylinders in a stagnant fluid. They use a thermal circuit with complicated algebra that is solved numerically by determining the resistance to the flow of energy.

Many of the thermal conductivities that have been obtained experimentally are currently available. Some of the better compilations are Cheng and Vachon [16], Luikov, et al. [6], Ofuchi and Kunii [17], and Krupiczka [7]. However, the experimental data appear to have deficiencies in that there is no data for systems with $\gamma < 1$ and only a limited amount of date for $\gamma = 0(1)$ systems. Most of the data available are for systems where γ is large. For systems where γ is small or of order one, it is recommended that experiments be run to determine the thermal conductivity.

After completing this review of models developed for predicting thermal conductivity in a porous medium, it is apparent that there is no acceptable general model. Some models have been shown to be acceptable in some special cases. Cheng and Vachon [16] have shown that most all of the commonly models used give results that differ by more than ten percent with experimentally determined thermal conductivities. This points toward the need to develop an acceptable general model for determining the effective thermal conductivity of porous media.

1.3 Proposal Statement

The objective of this study is to implement a general numerical model that can be used to determine the effective thermal conductivity of many different porous media geometries.

1.4 Summary

In this thesis, a numerical model based on the heat conduction model in Figure 9 will be developed by the superpositioning of a finite difference grid on a simulated porous medium. This porous medium is generated using a random number generator and will be composed of either solid or fluid elements. The ensuing difference equations will be solved utilizing the Alternating Direction Implicit (ADI) method. Employment of the ADI method begins by introducing a quasi-time derivative represented by stepping first in the x-direction ($k+^1/_2$ iteration) and then in the y-direction (k or k+1 iteration). Further manipulation will yield a series of N equations with N unknowns that can be solved using a Gaussian elimination method. The heat flux is then averaged in the x-direction, thus leading to determining the effective thermal conductivity.

This thesis continues next with the presentation of the method of solution followed by the results and discussion, and finishes with recommendations and conclusions.

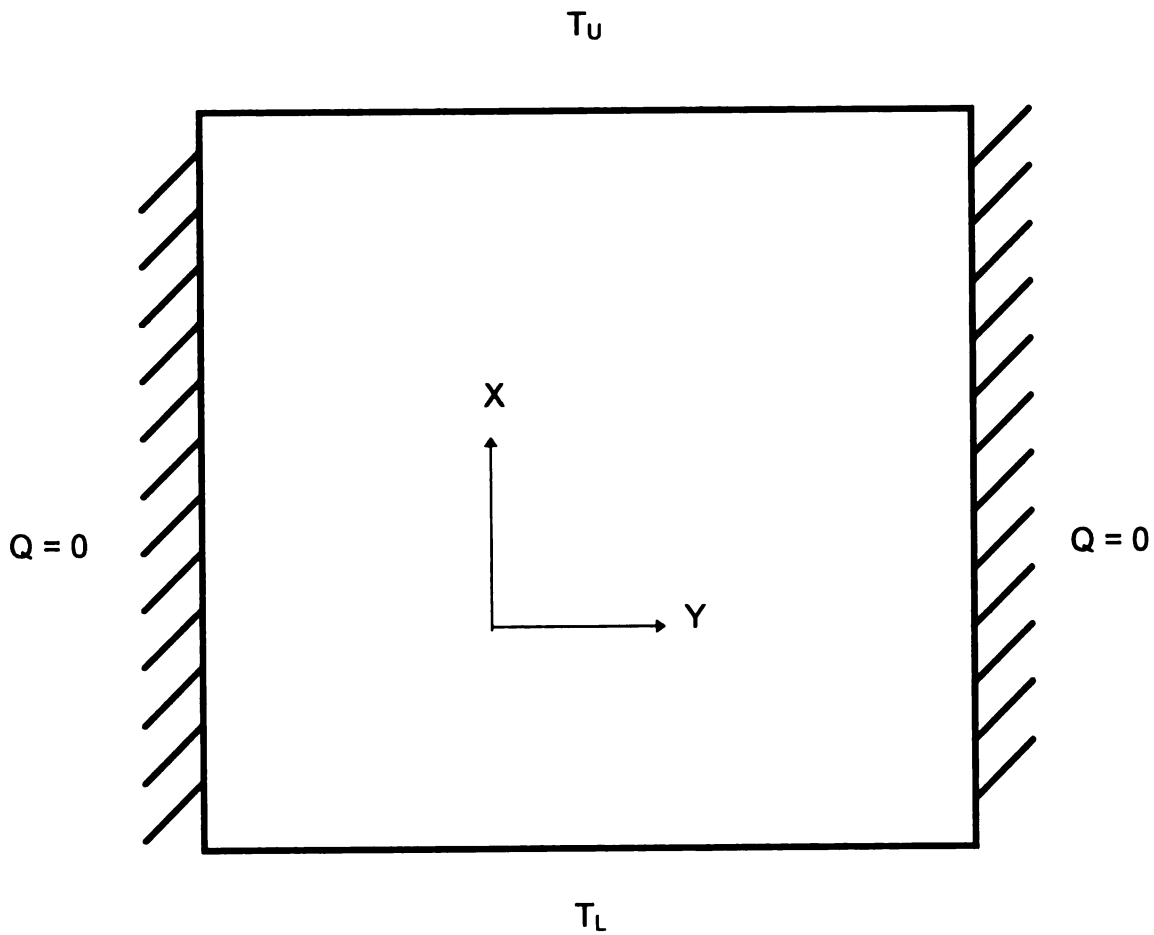

Figure 9. Heat Conduction Model

CHAPTER II

METHOD OF SOLUTION

2.1 Governing Equations

A porous medium can be arranged from a series of cylinders as shown in Figure 10. If a square grid is imposed over the porous media, then a grid that is fine enough to have single elements that are either a solid or a fluid can be visualized as in Figure 11. From this, a simulated porous medium can be generated. By placing a finite difference grid over this porous medium grid, a finite difference algorithm can be employed to solve the ensuing heat conduction problem. From this, the effective thermal conductivity can be determined for the entire porous medium.

The porous medium is generated by first determining a porosity to be used for the porous medium. Once a porosity value is decided upon, a random number between zero and one is generated and assigned to each element in the grid. Those elements assigned a random number less than the porosity value are fluid elements and those elements with a random number greater than the porosity value are solid elements.

Once the generated porous media grid is in place, the solution for the two dimensional heat conduction equation for the grid may be considered. The following equation may be written for each element as shown in Figure 12:

$$k_1^{(i)} \frac{\partial^2 T}{\partial x^2} + k_2^{(i)} \frac{\partial^2 T}{\partial y^2} = 0. \qquad (18)$$

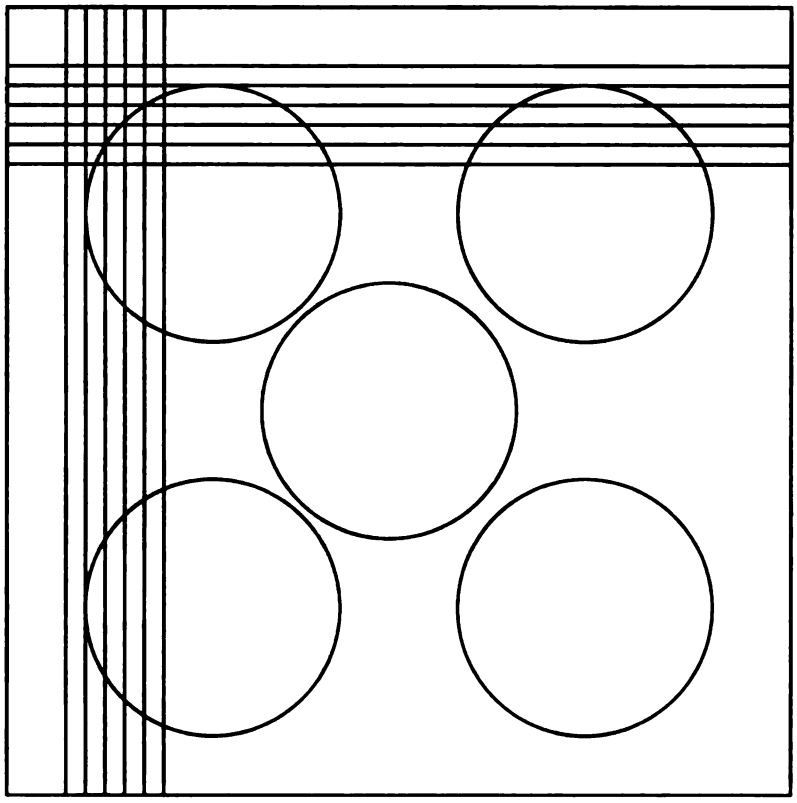

Figure 10. Array of Cylinders with Imposed Finite Element Grid

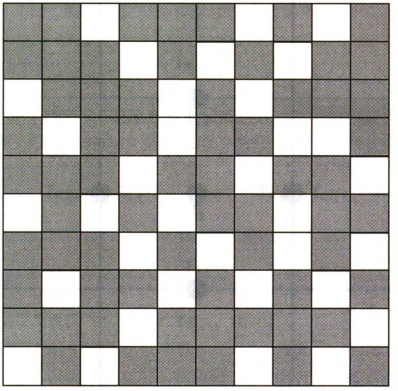

Figure 11. Simulated Porous Media Where
Shaded Area Represents Solid

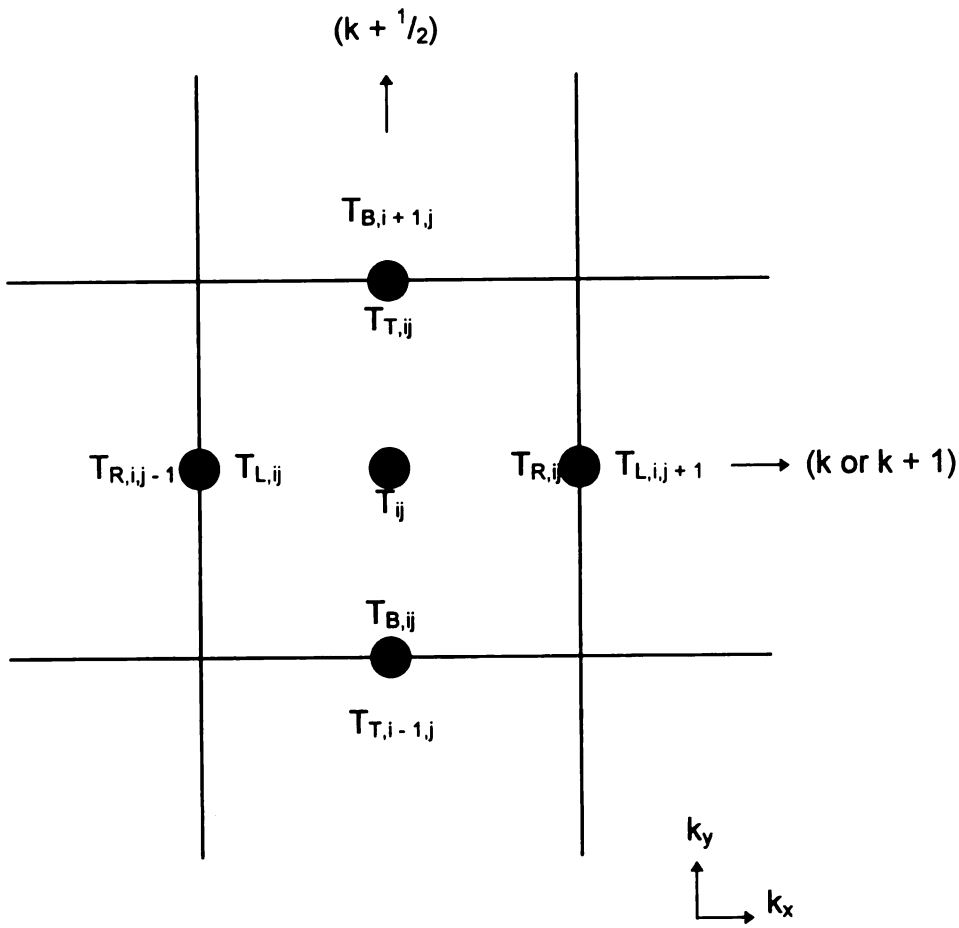

Figure 12. Finite Difference Element

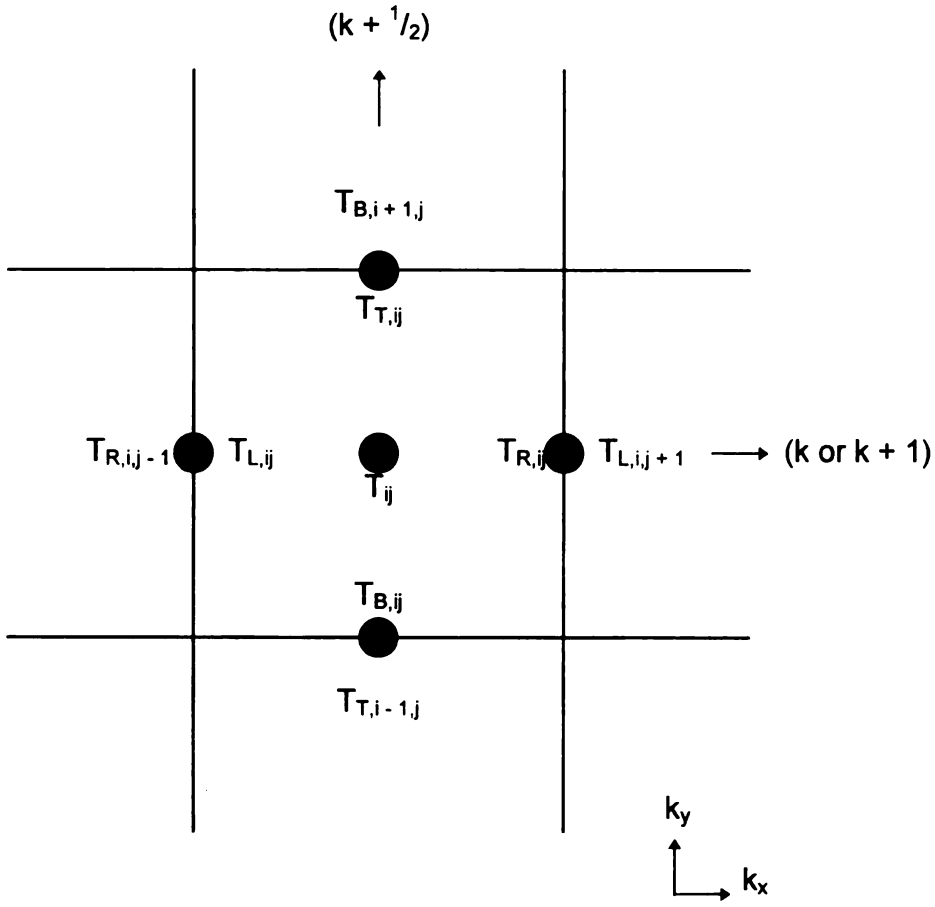

Figure 12. Finite Difference Element

The superscript i on the thermal conductivity indicates whether an element is to be either a solid (s) or a fluid (f) and the subscript indicates thermal conductivity as directionally dependent. The upper boundary is set at some temperature, T_U, and the lower boundary at some temperature, T_L, where $T_U > T_L$. Further, the sidewalls in the porous system will be considered to be adiabatic (Q = 0). Applying finite difference to Equation (18), the terms in Equation 18 become

$$\frac{\partial^2 T}{\partial x^2} = \frac{\left(T_{L,ij} - 2T_{ij} + T_{R,ij}\right)}{\left(\Delta x^2\right)} \tag{19}$$

and

$$\frac{\partial^2 T}{\partial y^2} = \frac{\left(T_{B,ij} - 2T_{ij} + T_{T,ij}\right)}{\left(\Delta y^2\right)}. \tag{20}$$

Substituting Equations (19) and (20) into Equation (18), we can write Equation (18) in the finite difference form

$$k^{(i)}_{x,ij}\left(\frac{T_{L,ij} - 2T_{ij} + T_{R,ij}}{\Delta x^2}\right) + k^{(i)}_{y,ij}\left(\frac{T_{B,ij} - 2T_{ij} + T_{T,ij}}{\Delta y^2}\right) = 0. \tag{21}$$

Now, the Alternating Direction Implicit (ADI) method will be utilized to solve the set of equations represented in Equation (21). To employ the ADI method, we must first set a quasi-time derivative that corresponds to first stepping in the y-direction (k + $^1/_2$ iterate) and then in the x-direction (k + 1 or k iterate).

The following equation is thus obtained:

$$T_{ij}^{(k+1/2)} - T_{ij}^{(k)} = \frac{k_{x,ij}}{\sigma_T}\left(T_{L,ij}^{(k)} - 2T_{ij}^{(k)} + T_{R,ij}^{(k)}\right)$$

$$+ \frac{k_{y,ij}}{\sigma_T}\left(T_{B,ij}^{(k+1/2)} - 2T_{ij}^{(k+1/2)} + T_{T,ij}^{(k+1/2)}\right) \qquad (22)$$

where

$$\sigma_T = \frac{(\Delta x)^2}{\Delta t_T} = \frac{(\Delta y)^2}{\Delta t_T} = \frac{\Delta^2}{\Delta t_T} \; . \qquad (23)$$

Before the set of equations represented by Equation (22) can be solved, adjacent finite difference elements must be coupled. This is done by observing that

$$T_{T,ij} = T_{B,i+1,j} \qquad (24)$$

$$T_{B,ij} = T_{T,i-1,j} \qquad (25)$$

$$T_{L,ij} = T_{R,i,j-1} \qquad (26)$$

$$T_{R,ij} = T_{L,i,j+1} \qquad (27)$$

which represents the temperature continuity at the boundaries between adjacent elements. There is also a continuity of the heat flux at the boundaries between adjacent elements. Therefore, we can also write the following equation:

$$k_{y,ij}\frac{T_{T,ij} - T_{ij}}{\Delta/2} = k_{y,i+1,j}\frac{T_{i+1,j} - T_{B,i+1,j}}{\Delta/2} \; . \qquad (28)$$

Substituting Equation (24) into Equation (28) yields the equation

$$k_{y,ij}\frac{T_{T,ij} - T_{ij}}{\Delta/2} = k_{y,i+1,j}\frac{T_{i+1,j} - T_{T,ij}}{\Delta/2} \; , \qquad (29)$$

and solving for $T_{T,ij}$ gives

$$T_{T,ij} = \frac{k_{y,i+1,j}\, T_{i+1,j}^{(k+\frac{1}{2})} + k_{y,ij}\, T_{ij}^{(k+\frac{1}{2})}}{k_{y,i+1,j} + k_{y,ij}}. \tag{30}$$

Similarly, the terms $T_{B,ij}$, $T_{L,ij}$, and $T_{R,ij}$ can all be expressed in terms of $T_{i-1,j}$, $T_{i,j-1}$, and $T_{i,j+1}$ such that

$$T_{B,ij} = \frac{k_{y,i-1,j}\, T_{i-1,j}^{(k+\frac{1}{2})} + k_{y,ij}\, T_{ij}^{(k+\frac{1}{2})}}{k_{y,i-1,j} + k_{y,ij}} \tag{31}$$

$$T_{L,ij} = \frac{k_{x,i,j-1}\, T_{i,j-1}^{(K)} + k_{x,ij}\, T_{ij}^{(k)}}{k_{x,i,j-1} + k_{x,ij}} \tag{32}$$

$$T_{R,ij} = \frac{k_{x,i,j+1}\, T_{i,j+1}^{(K)} + k_{x,ij}\, T_{ij}^{(k)}}{k_{x,i,j+1} + k_{x,ij}} \tag{33}$$

respectively. Substituting Equations (30), (31), (32), and (33) into Equation (22) yields the equation

$$\begin{aligned} &T_{ij}^{(k+\frac{1}{2})} - T_{ij}^{(k)} \\ &= \frac{k_{x,ij}}{\sigma_T}\left(\frac{k_{x,i-1,j}T_{i-1,j}^{(k)} + k_{x,ij}T_{ij}^{(k)}}{k_{x,i-1,j} + k_{x,ij}} - 2T_{ij}^{(k)} + \frac{k_{x,i+1,j}\, T_{i+1,j}^{(k)} + k_{x,ij}T_{ij}^{(k)}}{k_{x,i+1,j} + k_{x,ij}}\right) \\ &+ \frac{k_{y,ij}}{\sigma_T}\left(\frac{k_{y,i,j-1}T_{i,j-1}^{(k+\frac{1}{2})} + k_{y,ij}T_{ij}^{(k+\frac{1}{2})}}{k_{y,i,j-1} + k_{y,ij}} - 2T_{ij}^{(k+\frac{1}{2})} + \frac{k_{y,i,j+1}T_{i,j+1}^{(k+\frac{1}{2})} + k_{y,ij}T_{ij}^{(k+\frac{1}{2})}}{k_{y,i,j+1} + k_{y,ij}}\right). \end{aligned} \tag{34}$$

By rewriting Equation (34) and collecting the coefficients on each element temperature, T, the coefficients can be written for

$$T_{i,j-1}^{(k+\frac{1}{2})}: \quad B_{ij} = -\frac{k_{y,ij}\, k_{y,i,j-1}}{\sigma_T\left(k_{y,ij} + k_{y,i,j-1}\right)}, \tag{35}$$

$$T_{ij}^{(k+1/2)}:\ C_{ij} = 1 - \frac{k_{y,ij}^2}{\sigma_T\left(k_{y,ij} + k_{y,i,j-1}\right)} - \frac{k_{y,ij}^2}{\sigma_T\left(k_{y,ij} + k_{y,i,j+1}\right)} + 2\frac{k_{y,ij}}{\sigma_T}, \tag{36}$$

$$T_{i,j+1}^{(k+1/2)}:\ D_{ij} = -\frac{k_{y,ij}\, k_{y,i,j+1}}{\sigma_T\left(k_{y,ij} + k_{y,i,j+1}\right)}, \tag{37}$$

$$T_{i-1,j}^{(k)}:\ E_{ij} = \frac{k_{x,ij}\, k_{x,i-1,j}}{\sigma_T\left(k_{x,ij} + k_{x,i-1,j}\right)}, \tag{38}$$

$$T_{ij}^{(k)}:\ F_{ij} = 1 + \frac{k_{x,ij}^2}{\sigma_T\left(k_{x,ij} + k_{x,i-1,j}\right)} + \frac{k_{x,ij}^2}{\sigma_T\left(k_{x,ij} + k_{x,i+1,j}\right)} - 2\frac{k_{x,ij}}{\sigma_T}, \tag{39}$$

$$T_{i+1,j}^{(k)}:\ G_{ij} = \frac{k_{x,ij}\, k_{x,i+1,j}}{\sigma_T\left(k_{x,ij} + k_{x,i+1,j}\right)}, \tag{40}$$

and the following equation can be written

$$B_{ij}\, T_{i,j-1}^{(k+1/2)} + C_{ij}\, T_{ij}^{(k+1/2)} + D_{ij}\, T_{i,j+1}^{(k+1/2)} = E_{ij}\, T_{i-1,j}^{(k)} + F_{ij}\, T_{ij}^{(k)} + G_{ij}\, T_{i+1,j}^{(k)} \tag{41}$$

Further, Equation (41) can be written as a set of equations

$$\overline{\overline{M}}_j^{(k+1/2)}\, \overline{T}_j^{(k+1/2)} = \overline{S}^{(k)} \tag{42}$$

where $\overline{\overline{M}}_j^{(k+1/2)}$ is represented by a tridiagonal matrix. By employing a Gaussian elimination routine called the *Thomas algorithm* , Equation (42) can be solved for $\overline{T}_j^{(k+1/2)}$. This routine has the advantage of being able to store the required coefficients in a compact 3 x N^2 matrix. This is done as j is stepped form 1 to N. Similarly, an equation can be developed for the k + 1 iteration and solving for

$\bar{T}_i^{(k+1)}$ as i is stepped from 1 to N. The solutions are obtained alternately in each direction iteratively until the solutions converge.

2.2 Boundary Conditions

It is observed that at the left boundary, where the adiabatic walls exist, the heat flux equation becomes

$$\left.\frac{\partial T}{\partial x}\right|_{x=0} = 0 \tag{43}$$

which becomes

$$\frac{T_R - T_L}{\Delta x} = 0. \tag{44}$$

Therefore,

$$T_L = T_R. \tag{45}$$

Equation (45) is then substituted into Equation (22) to obtain

$$T_{ij}^{(k+\frac{1}{2})} - T_{ij}^{(k)} = \frac{k_{x,ij}}{\sigma_T}\left(2T_{L,ij}^{(k)} - 2T_{ij}^{(k)}\right) + \frac{k_{y,ij}}{\sigma_T}\left(T_{B,ij}^{(k+\frac{1}{2})} - 2T_{ij}^{(k+\frac{1}{2})} + T_{T,ij}^{(k+\frac{1}{2})}\right) \tag{46}$$

Similarly, the boundary condition at the right wall is

$$\left.\frac{\partial T}{\partial x}\right|_{x=N} = 0$$

and the finite difference equation becomes

$$T_{ij}^{(k+\frac{1}{2})} - T_{ij}^{(k)} = \frac{k_{x,ij}}{\sigma_T}\left(2T_{R,ij}^{(k)} - 2T_{ij}^{(k)}\right)$$

$$+ \frac{k_{y,ij}}{\sigma_T}\left(T_{B,ij}^{(k+\frac{1}{2})} - 2T_{ij}^{(k+\frac{1}{2})} + T_{T,ij}^{(k+\frac{1}{2})}\right). \quad (47)$$

The B,C,D,E,F, and G coefficients are then obtained as before. In addition, the initial condition at the bottom of the porous medium is

$$T_{B,i1} = T_L \quad (48)$$

and at the top, the initial condition is

$$T_{T,iN} = T_U. \quad (49)$$

The B, C, D, E, F, and G coefficients are then again obtained as before.

The effective thermal conductivity can be obtained by determining the average heat flux in the y-direction while x = 0

$$\bar{q} = \frac{1}{N}\sum_{i=1}^{N} k_{y,i,j=0}\left.\frac{\partial T}{\partial y}\right|_{i,j=0} \quad (47)$$

and then applying the definition from Equation (1) and assuming L = 1,

$$k_m = \frac{\bar{q}}{\Delta T}. \quad (48)$$

CHAPTER III

RESULTS AND DISCUSSION

3.1 Porous Media Generation

The porous media generation is accomplished by the use of the pseudo-random number generator function call available in Microsoft FORTRAN. Figure 13 shows the results of running the random number generator one hundred times for each porosity from 0.1 to 0.9. The values are then normalized by dividing the generated porosity by the target porosity. For example, with a target porosity of 0.1, the calculated porosities range from 0.04 to 0.18 with a population standard deviation of 0.027. This distribution is shown in Figure 14. This results in a normalized porosity of 0.4 to 1.8. Further, running the random number generator for a target porosity of 0.9 results in a range from 0.83 to 0.96 with a population standard deviation of 0.026 giving a normalized porosity of 0.92 to 1.07. This distribution is shown in Figure 15. As will be seen in the discussion on numerical testing, the randomness of the generated porous media will result in slight deviations as the different data are put into graphical form.

Figure 16 shows calculated porosity as a function of grid size. A thermal conductivity of 0.3 was used. As before, the actual porosities tend toward the target porosities of 0.3, 0.5, and 0.8 as the grid size is increased.

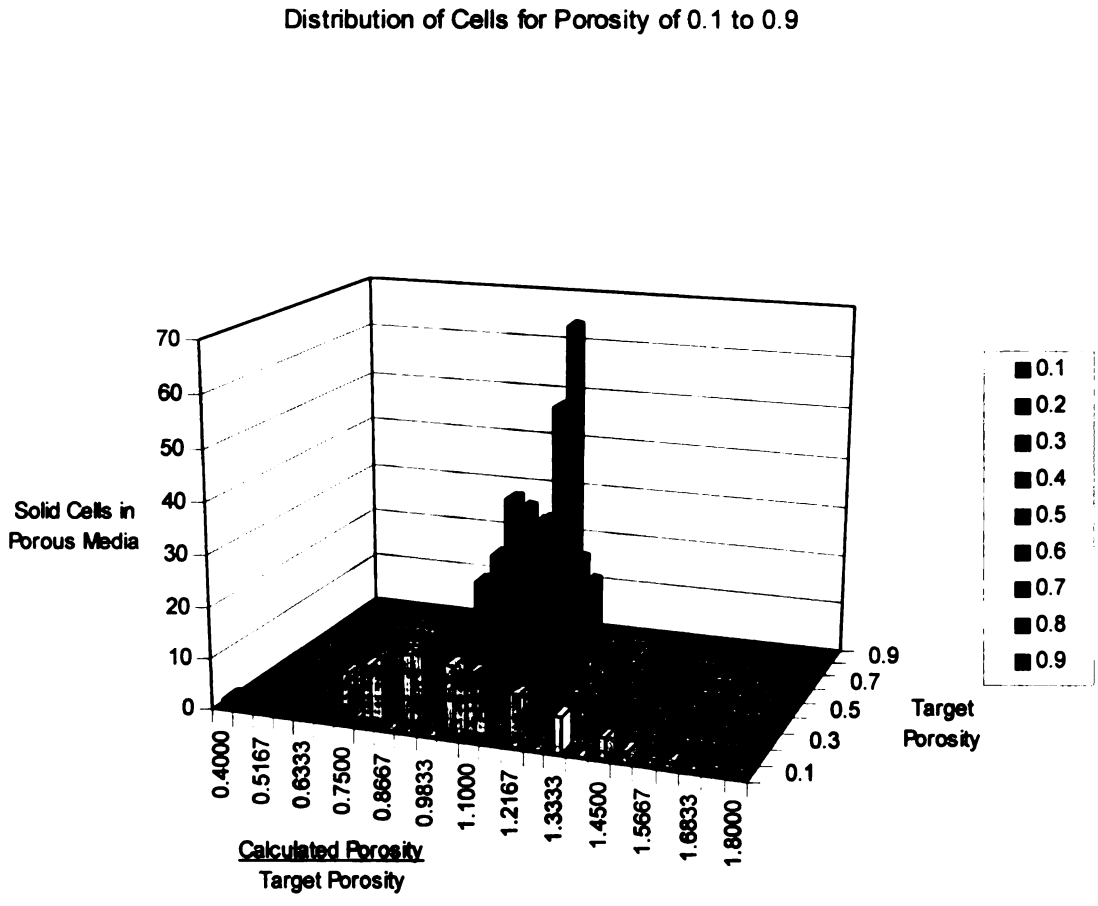

Figure 13. Normalized Porosity for Target Porostiy of 0.1 to 0.9

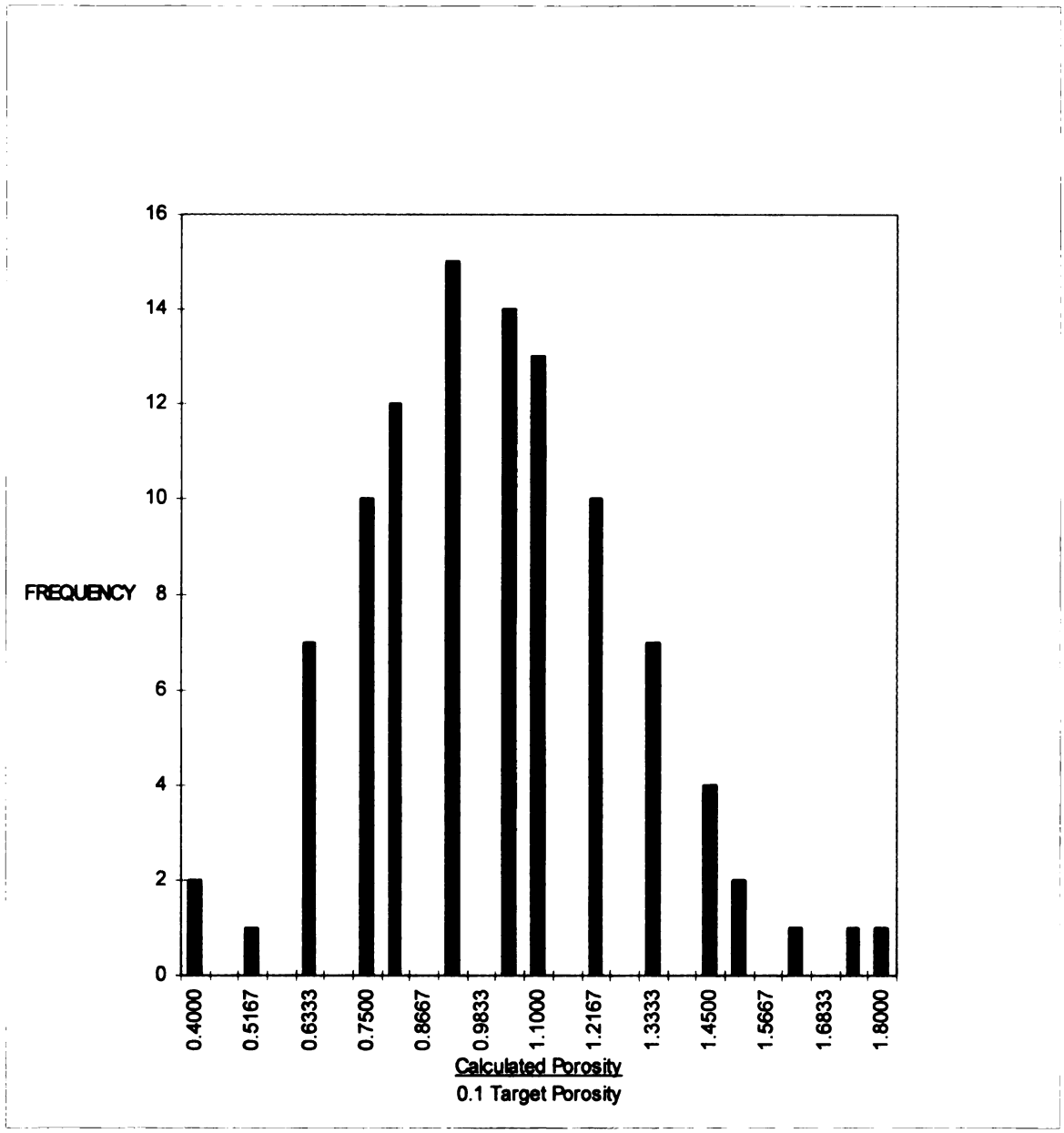

Figure 14. Frequency vs. 0.1 Normalized Porosity

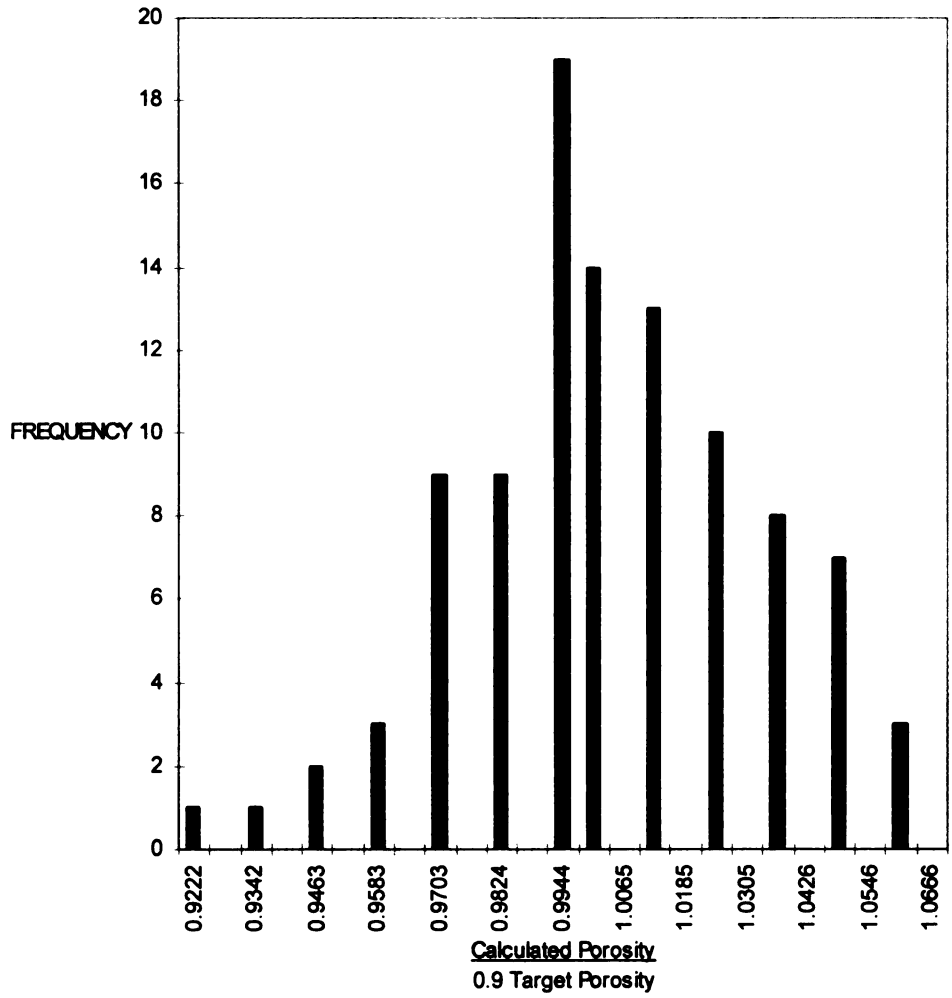

Figure 15. Frequency vs. 0.9 Normalized Porosity

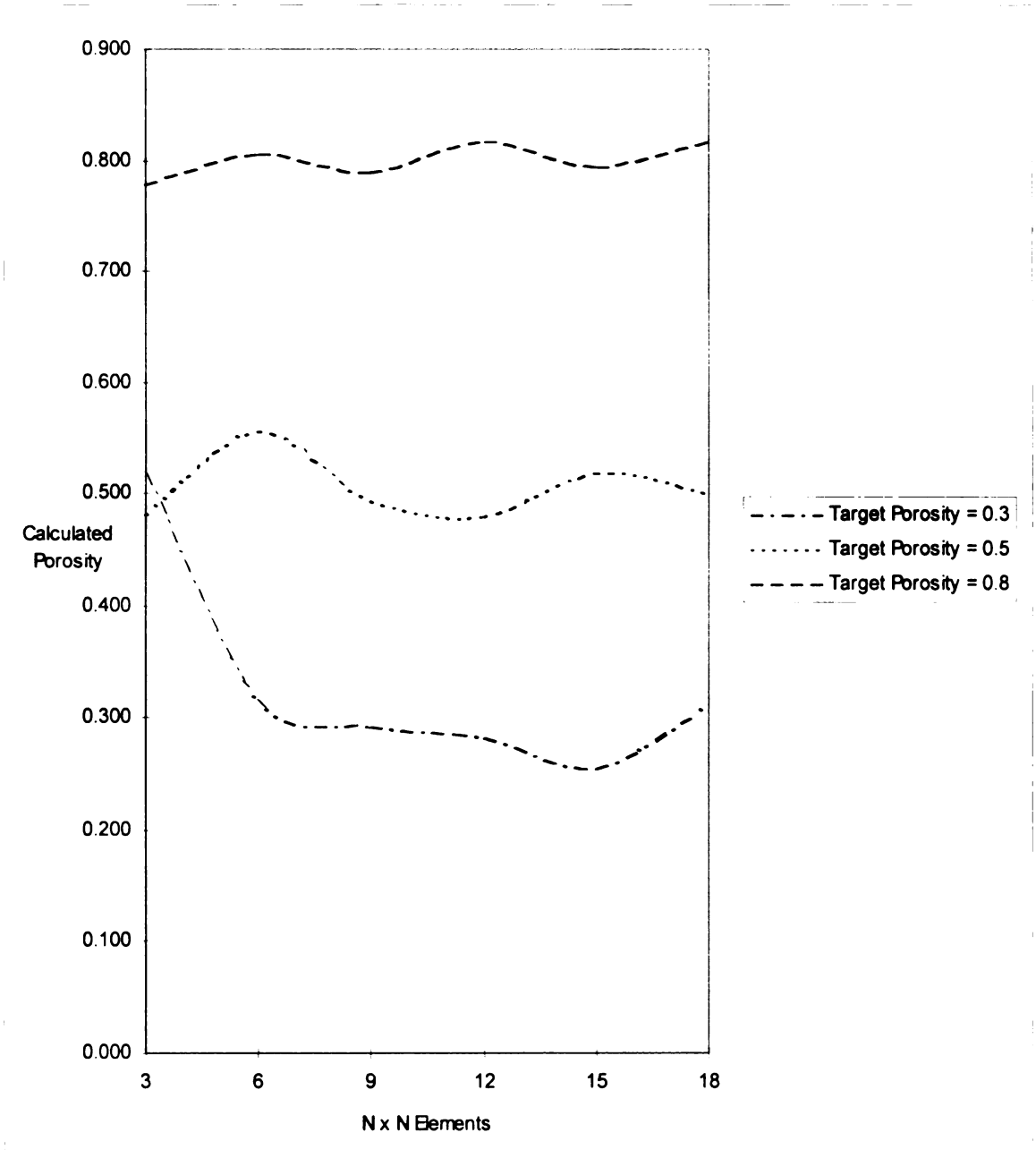

Figure 16. Calculated porosity vs. N x N Elements

Further, it is expected that as the grid size increases, the calculated porosity will converge around a single value as determined by the set target porosity. This is confirmed by the graph in Figure 17 which represents the calculated porosity as a function of grid size. Figure 18 shows that for a k_f/k_s = 0.5 (0.3/0.6) and a DT = 0.1, the effective thermal conductivity will approach a single value as the grid size is increased.

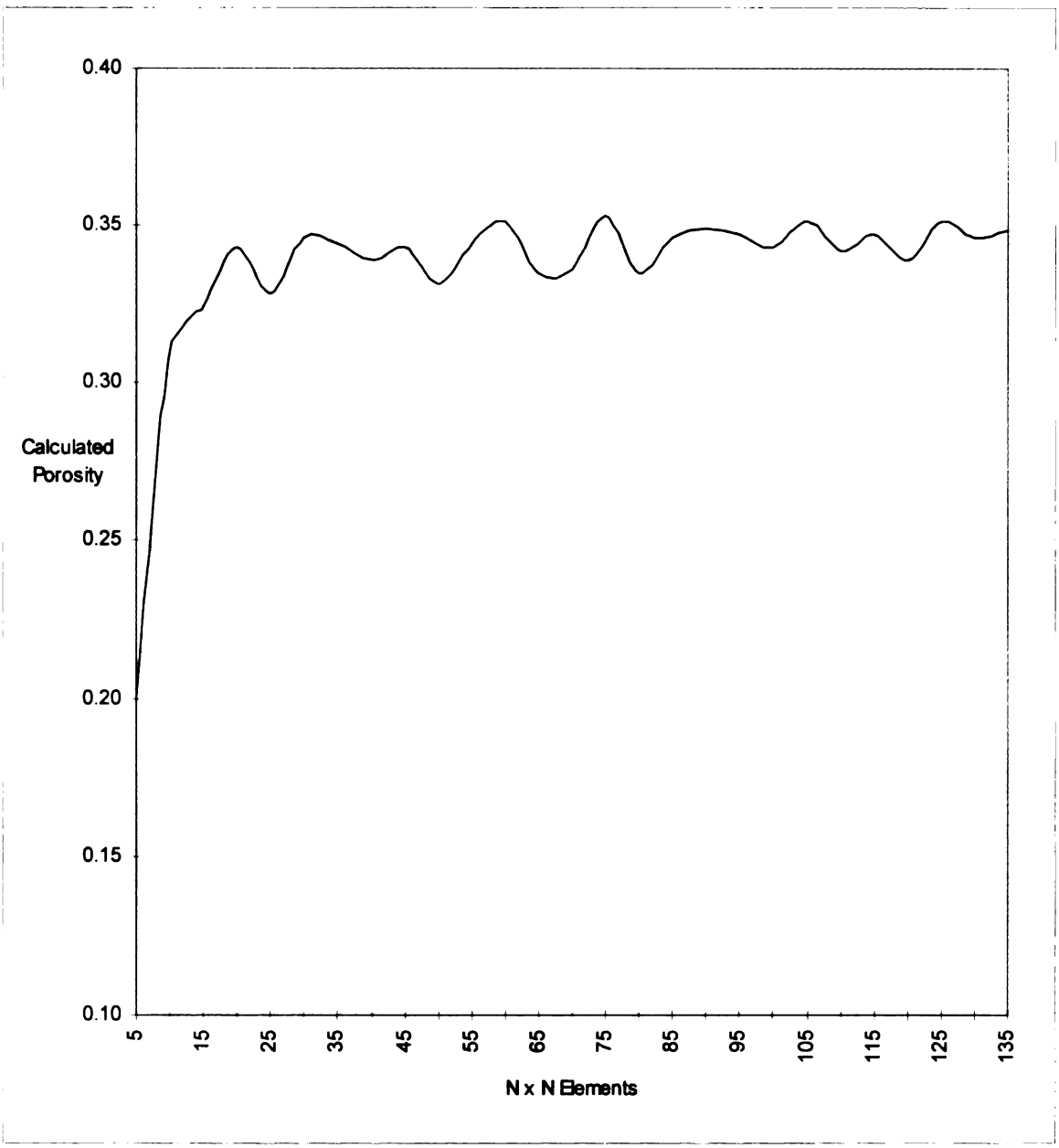

Figure 17. Calculated porosity vs. N x N Elements

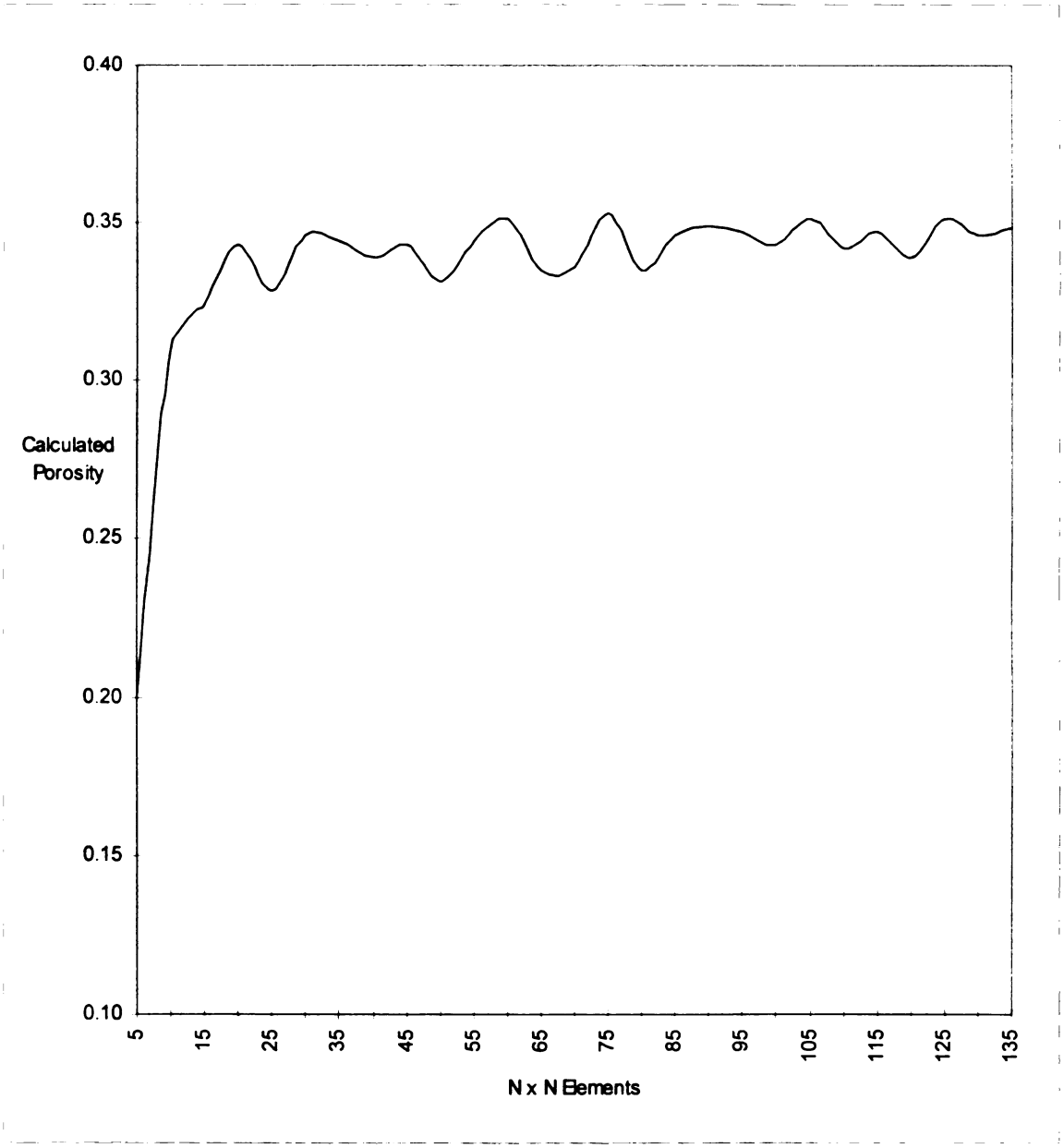

Figure 17. Calculated porosity vs. N x N Elements

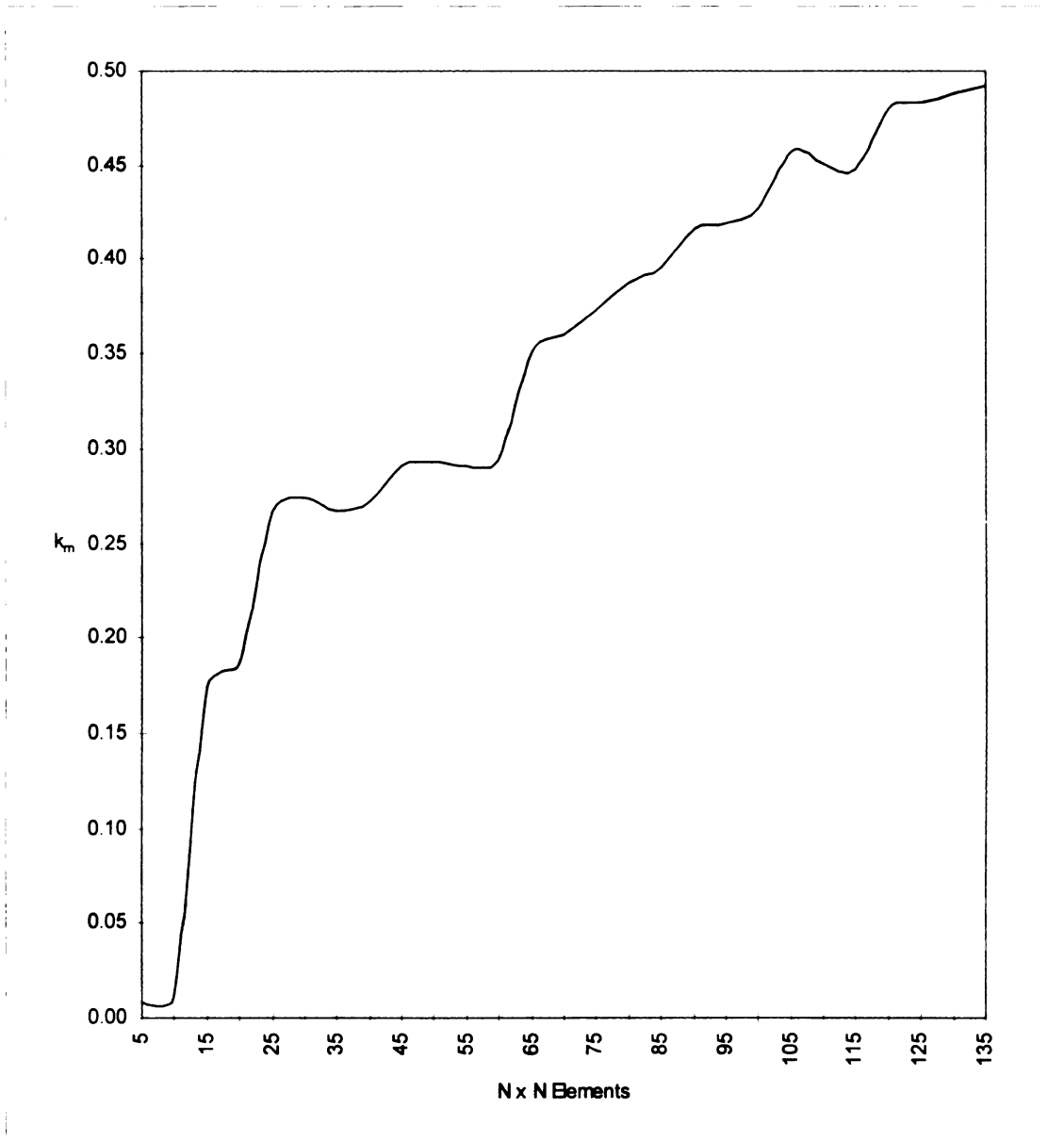

Figure 18. Effective Thermal Conductivity vs. N x N Elements

3.2 Results of Numerical Validation

For the following numerical testing, a target porosity of 0.3456 was used unless specifically stated otherwise. Thermal conductivity values of either 0.3 or 0.03 were used for the fluid and solid materials in the following numerical tests. Figure 19, showing effective thermal conductivity as a function of the grid size, indicates the relative range of thermal conductivities for k_f/k_s of 0.1, 1.0, and 10.0. As expected, these curves trend closer to one value as the grid size is increased.

In Figure 20, the effective thermal conductivity is plotted as a function of the $\log_{10}$ of the time step. As before, thermal conductivities of either 0.3 and 0.03 were used for the fluid and solid materials. These graphs were expected to converge around one value as the time step is increased. The fluctuation that is seen is attributed to the randomness of the grid generation. However, these curves do tend toward a central value. Figure 21 shows the effective thermal conductivity as a function of the target porosity for thermal conductivity ratios of 0.5, 1.0, and 2.0 using thermal conductivities of 0.3 and 0.6. These curves also behave as expected. When $k_f/k_s = 2.0$ at a target porosity of 0.0 to 1.0, the curve is equal to 0.3 and 0.6 respectively, and when $k_f/k_s = 0.5$ with the target porosity once again running from 0.0 to 1.0, the curve runs from 0.6 to 0.3 respectively. This is also the expected result. Finally, with $k_f/k_s = 1.0$ and the thermal conductivities set equal to 0.3, the curve is equal to 0.3 from a target porosity of 0.0 to 1.0.

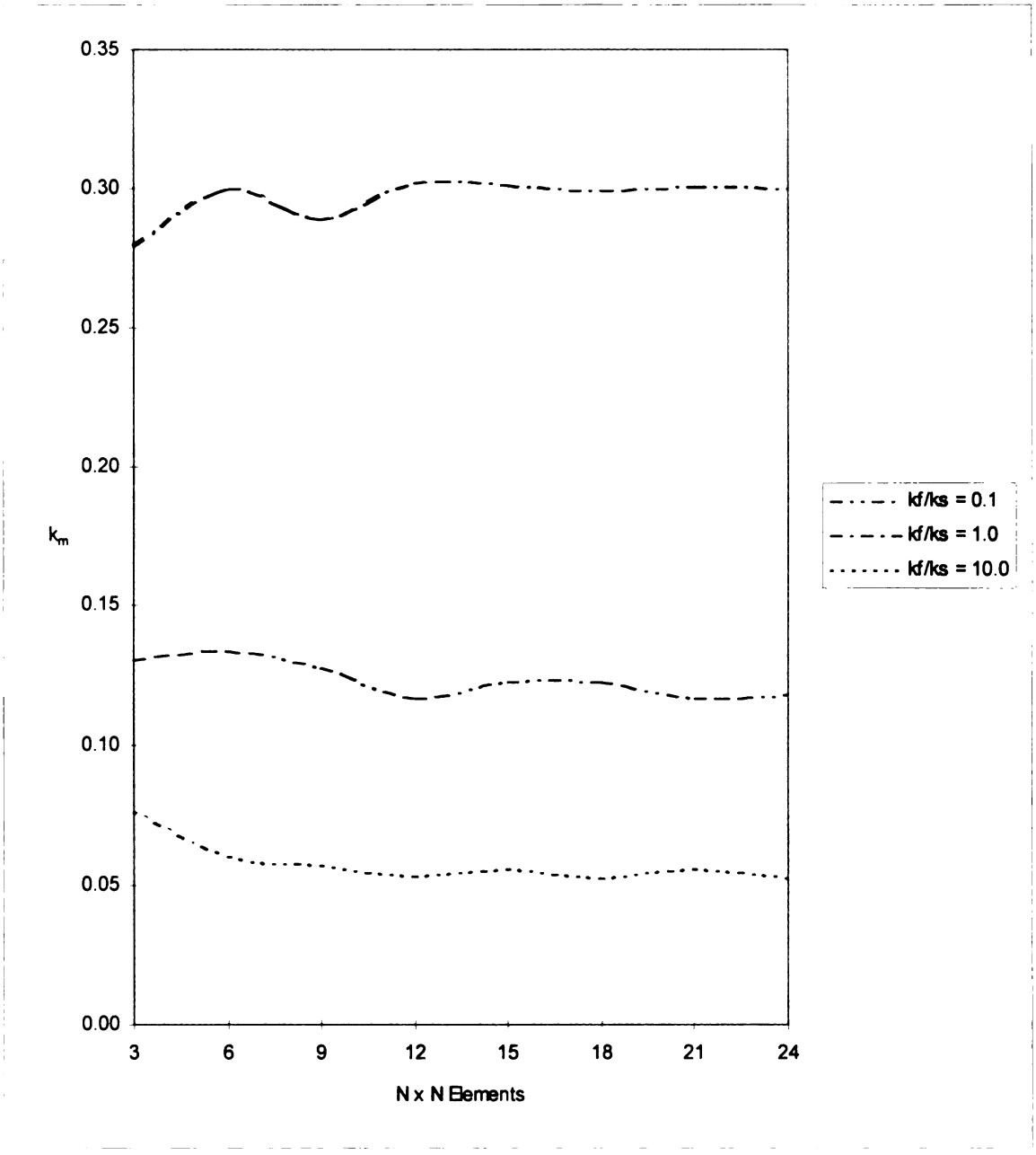

Figure 19. Effective Thermal Conductivity vs. N x N Elements

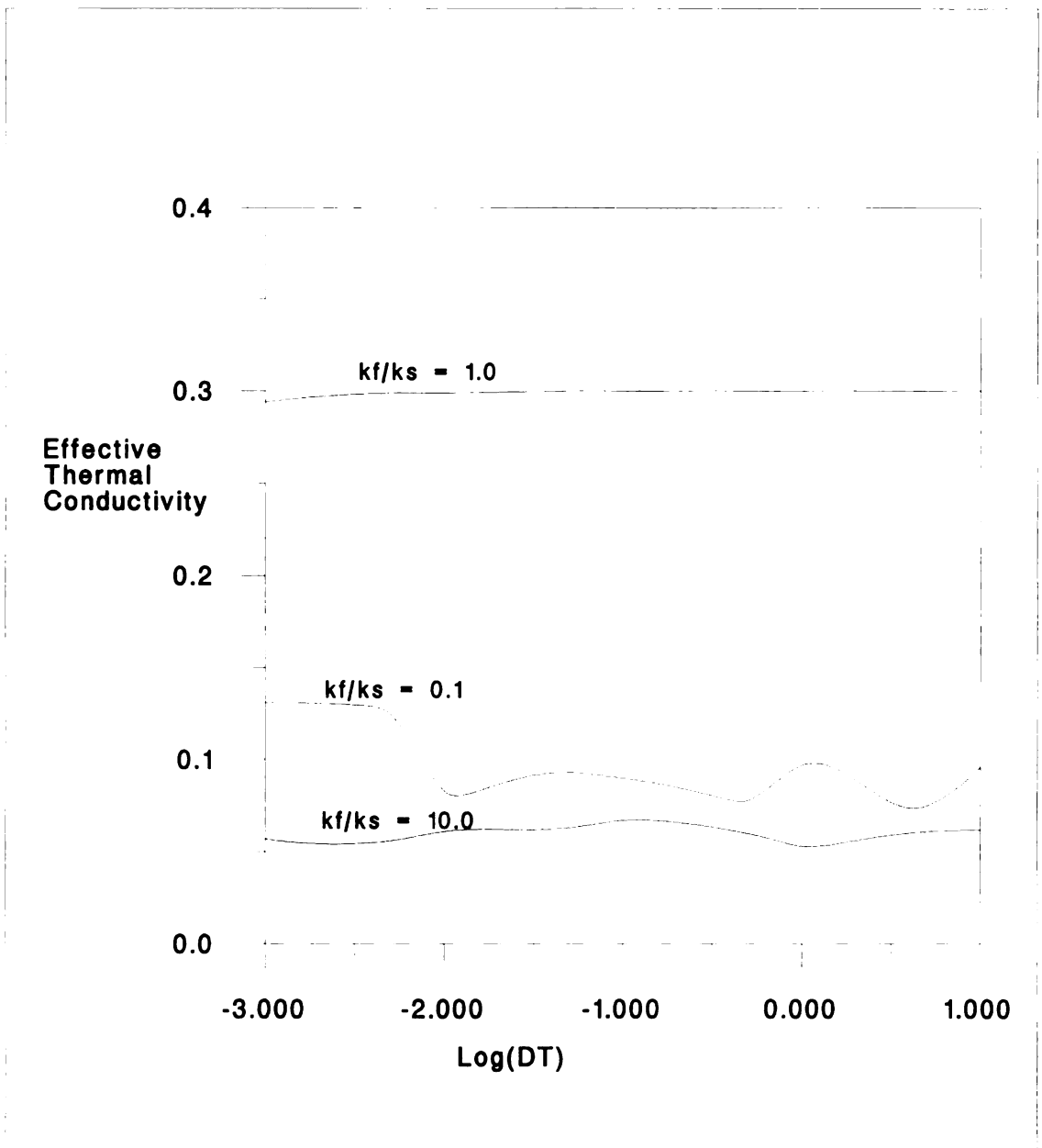

Figure 20. Effective Thermal Conductivity vs. Log (DT)

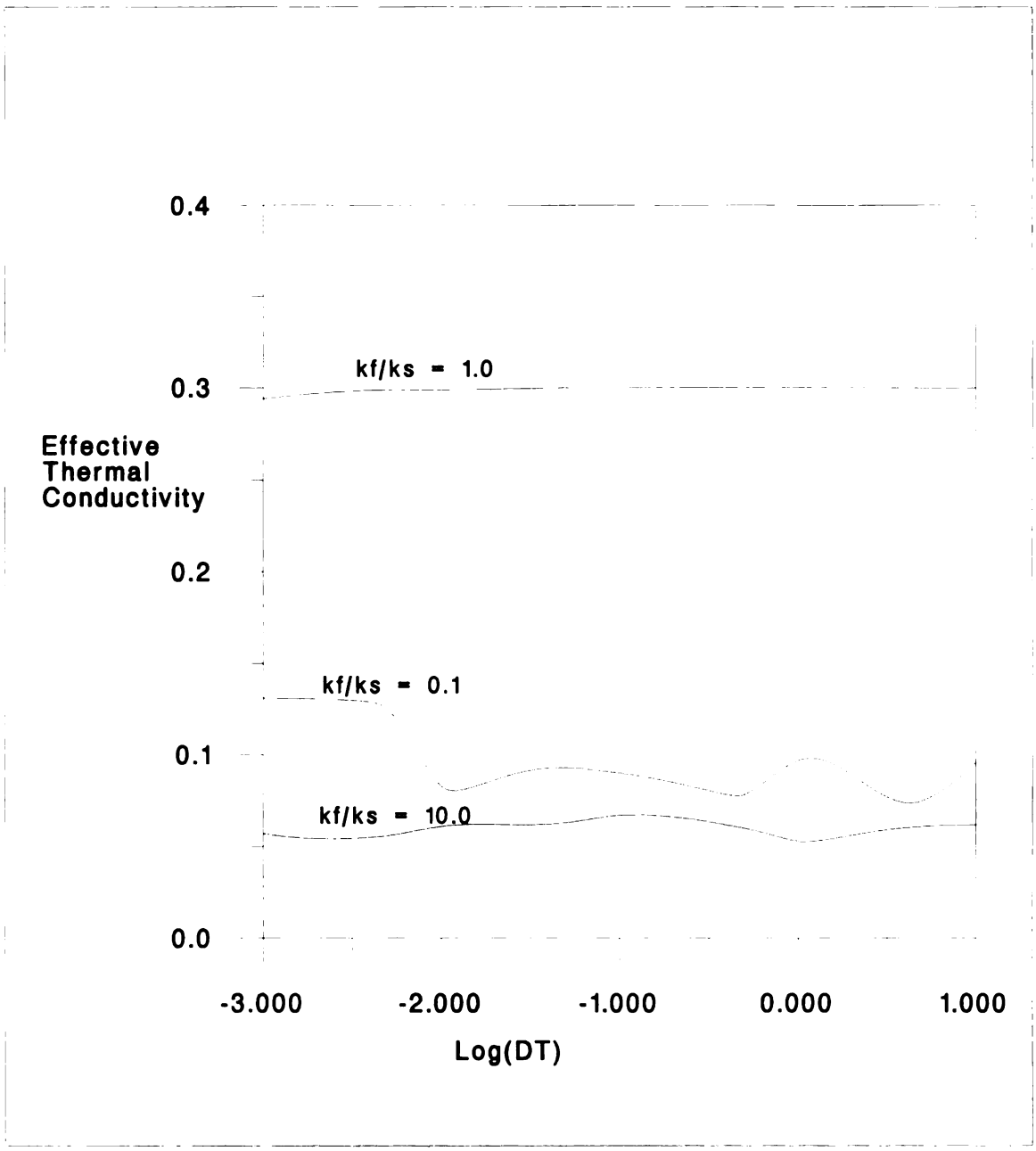

Figure 20. Effective Thermal Conductivity vs. Log (DT)

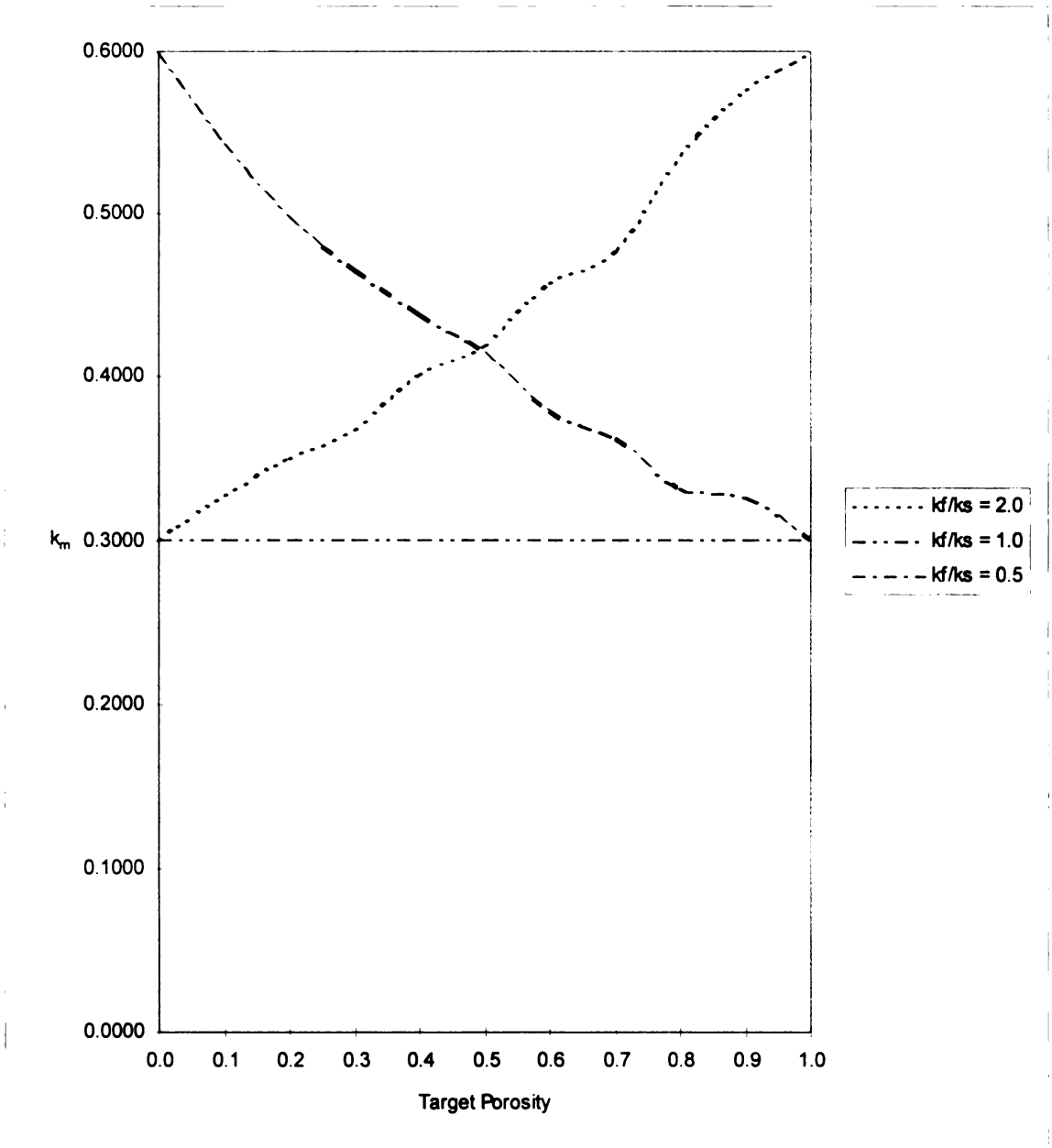

Figure 21. Effective Thermal Conductivity vs. Target Porosity

The three curves in Figure 22 show the effective thermal conductivity for k_f^x/k_s^x = 0.1, k_f^x/k_f^y = 1.0, k_s^x = constant and k_s^y being varied such that k_s^x/ k_s^y = 0.5, 1.0, and 2.0.

Finally, Figure 23 is the same graph as Figure 6 with an additional curve. The two curves in Figure 6 show the theoretical boundaries for porous media. The one curve being the graphical representation of the parallel model and the other curve being the graphical representation of the series model. The third curve in Figure 22 represents the model as proposed in this paper. The shape to the curve is due to the random generation of the fluid and solid cells in the porous medium. As stated previously, all current models for determining the effective thermal conductivity of a porous medium fall between the boundaries as established by the parallel and series models. As expected, Figure 22 shows that the curve for this model also lies between these two limits.

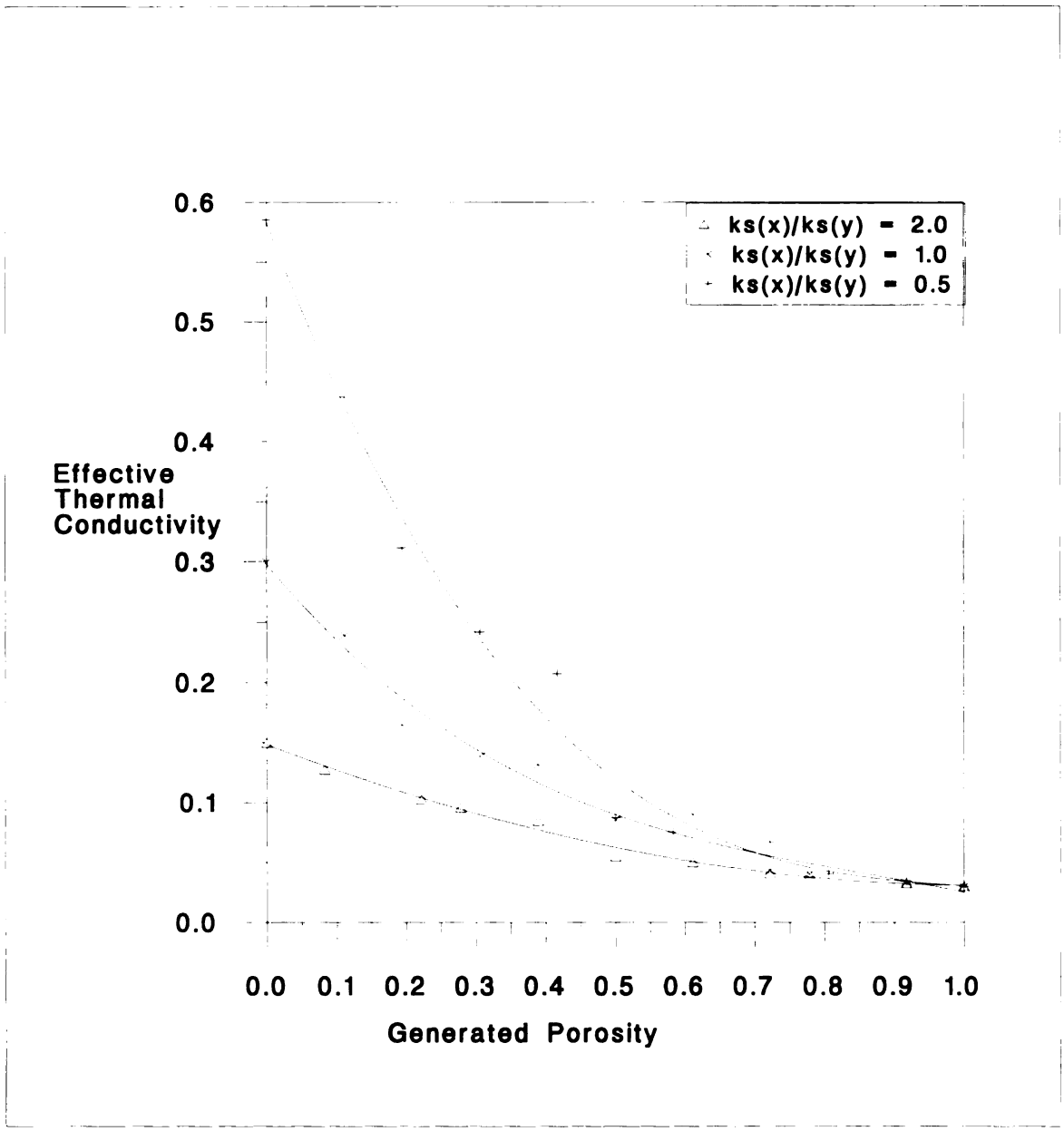

Figure 22. k_m vs. Generated Porosity

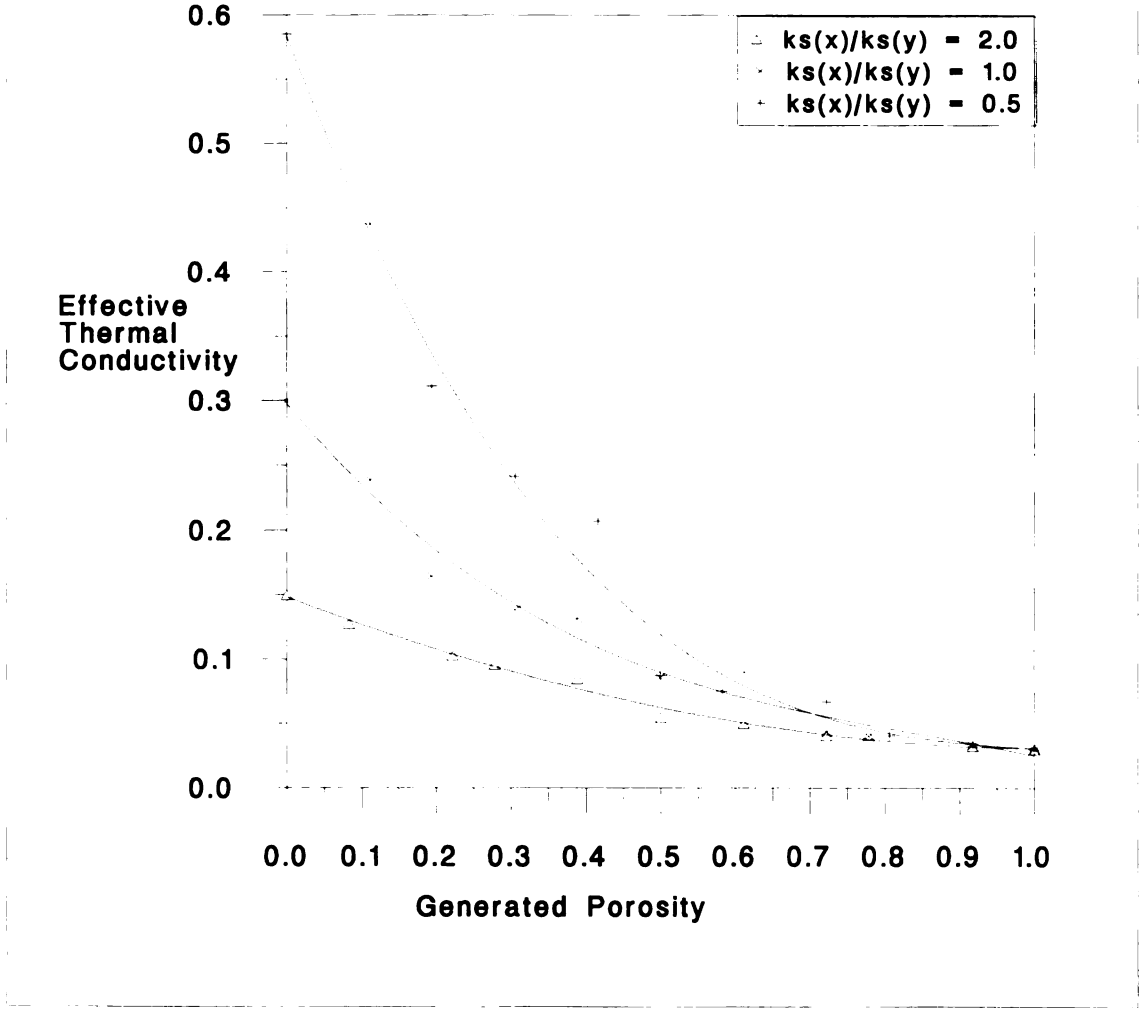

Figure 22. k_m vs. Generated Porosity

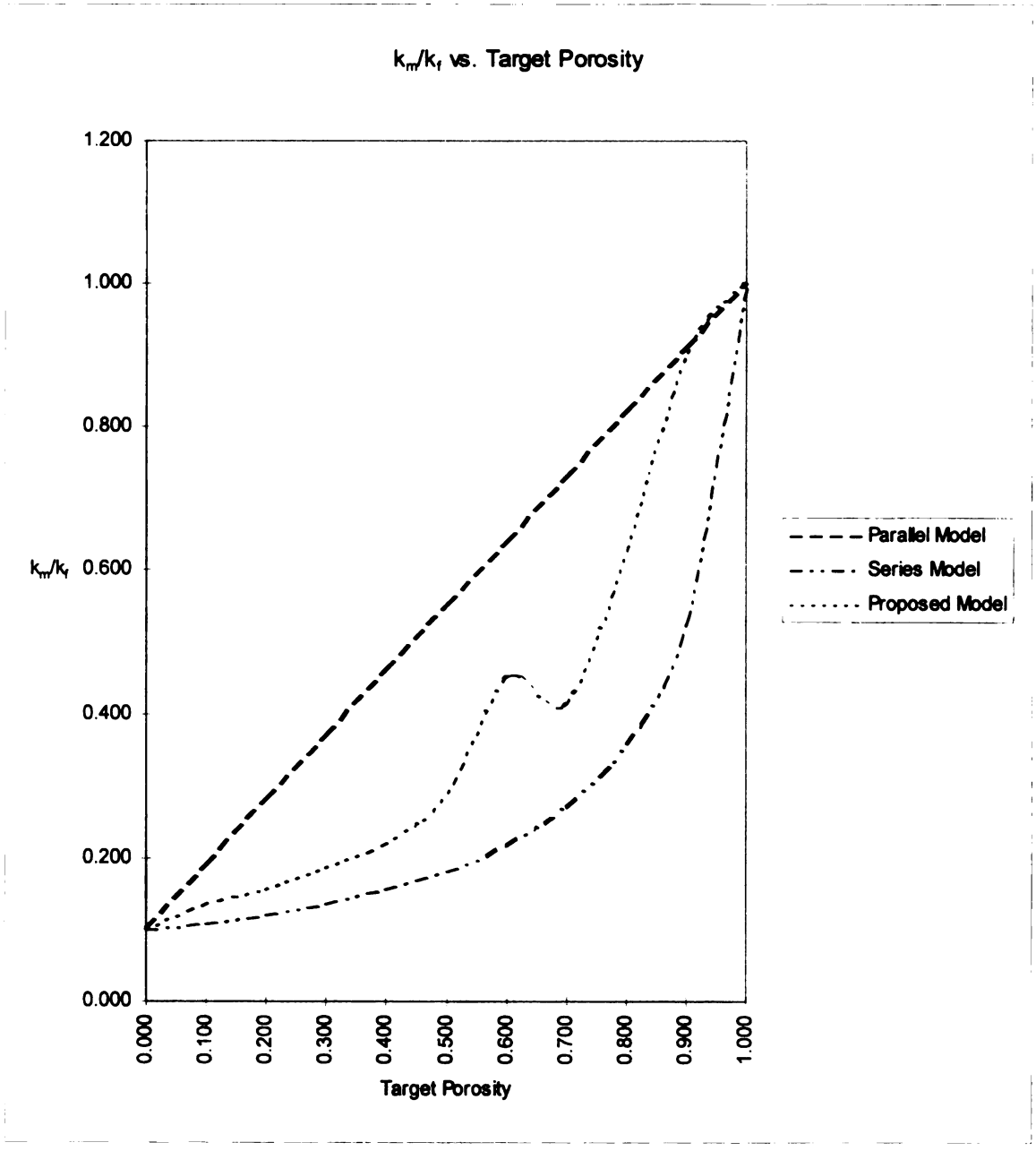

Figure 23. k_m/k_f vs. Target Porosity

CHAPTER IV

CONCLUSIONS AND RECOMMENDATIONS

4.1 Conclusions

1. As matrix size is increased the effective thermal conductivity will trend toward a close set of values that are dependent upon the chosen target porosity.

2. The effective thermal conductivity is well behaved between the set solid and fluid thermal conductivities for 0.0 target porosity to 1.0 target porosity.

3. The validity of this model is supported by the ratio of effective thermal conductivity to fluid thermal conductivity curve falling between the two theoretical boundaries of the series and the parallel model.

4. The calculated porosity does not necessarily match a specified target porosity due to the random generation of the porous medium grid.

4.2 Recommendations

1. The current program requires more substantial testing using materials with anisotropic properties.

2. The next extension of this numerical model would be to expand the capability to model three, four, five, or more components. This would allow for the determination of the effective thermal conductivity of systems consisting of multi-component materials.

3. Another refinement would be to utilize the Monte Carlo method for generating the material matrix. Each cell in the matrix would have an equal

opportunity of being assigned a value from one to N that would be used in determining whether that cell would be a fluid cell or a solid cell.

APPENDIX

APPENDIX

Sample output for kf = 0.3 and ks = 0.3, DT = 10 seconds, and convergence criteria set to 0.01 degrees.

RESULTS OF EFFECTIVE THERMAL CONDUCTIVITY CALCULATION

TARGET POROSITY:	0.346
GENERATED POROSITY:	0.361
GRID SIZE:	6
EFFECTIVE THERMAL CONDUCTIVITY:	2.999E-01
ITERATION COUNT:	2203

MATERIAL MATRIX:

2 2 1 1 1 2
1 2 1 1 2 1
1 1 1 1 2 1
1 1 2 1 2 2
2 2 1 2 1 2
1 1 1 1 1 1

TEMPERATURE FIELD:

345.8	345.8	345.8	345.8	345.8	345.8
337.5	337.5	337.5	337.5	337.5	337.5
329.2	329.2	329.2	329.2	329.2	329.2
320.8	320.8	320.8	320.8	320.8	320.8
312.5	312.5	312.5	312.5	312.5	312.5
304.2	304.2	304.2	304.2	304.2	304.2

Sample output for kf = 0.6 and ks = 0.3, DT = 10 seconds, and convergence criteria set to 0.01 degrees.

RESULTS OF EFFECTIVE THERMAL CONDUCTIVITY CALCULATION

TARGET POROSITY:	0.346
GENERATED POROSITY:	0.333
GRID SIZE:	6
EFFECTIVE THERMAL CONDUCTIVITY:	3.819E-01
ITERATION COUNT:	741

MATERIAL MATRIX:

2 2 1 2 1 1
1 2 1 1 2 2
1 2 2 1 1 1
2 1 1 2 1 1
1 1 1 1 1 1
1 1 2 1 2 1

TEMPERATURE FIELD:

345.9	346.1	345.8	345.5	345.4	345.0
337.5	338.5	337.2	336.3	336.7	336.8
329.0	329.4	327.8	328.2	328.5	328.6
319.8	319.5	319.2	320.4	320.4	320.6
311.2	311.9	312.6	311.5	312.2	312.9
304.0	304.6	304.6	303.3	303.9	304.2

Sample output for kf = 0.3 and ks = 0.6, DT = 10 seconds, and convergence criteria set to 0.01 degrees.

RESULTS OF EFFECTIVE THERMAL CONDUCTIVITY CALCULATION

TARGET POROSITY:	0.346
GENERATED POROSITY:	0.333
GRID SIZE:	6
EFFECTIVE THERMAL CONDUCTIVITY:	4.678E-01
ITERATION COUNT:	1123

MATERIAL MATRIX:

2 1 1 1 1 1
1 1 1 2 1 1
2 1 2 1 1 1
1 1 1 2 2 1
2 2 2 2 2 1
1 1 1 1 1 2

TEMPERATURE FIELD:

346.3	346.4	346.4	347.0	346.9	345.7
338.7	339.3	338.8	339.0	338.5	336.9
329.9	330.0	330.6	328.9	329.1	328.8
321.0	320.3	320.8	319.6	320.3	320.4
313.6	312.7	312.5	312.1	312.2	312.2
305.0	304.4	304.7	304.1	304.1	304.1

Sample output for kx(f) = 0.6, ky(f) = 0.3 and kx(s) = 0.2, ky(s) = 0.8, DT = 10 seconds, and convergence criteria set to 0.01 degrees.

RESULTS OF EFFECTIVE THERMAL CONDUCTIVITY CALCULATION

TARGET POROSITY:	0.346
GENERATED POROSITY:	0.278
GRID SIZE:	6
EFFECTIVE THERMAL CONDUCTIVITY:	5.991E-01
ITERATION COUNT:	3152

MATERIAL MATRIX:

2 1 1 2 1 1
1 1 1 1 1 2
2 2 2 1 1 1
1 1 1 1 2 1
2 1 1 1 2 1
1 1 1 1 1 2

TEMPERATURE FIELD:

345.9	344.5	345.9	347.0	346.7	344.5
338.7	335.1	338.0	336.7	336.0	333.9
328.9	328.4	331.2	326.5	325.9	326.6
319.7	320.7	322.2	319.9	320.0	319.6
314.2	312.7	312.9	312.4	314.3	312.5
305.4	304.4	304.3	304.3	305.4	304.4

LIST OF REFERENCES

Specific References

1. Baradat, y. and Combarnous, M., "Conductivite Thermique des Milieux Poreux," Institut Francais du Petrole, Bordeaus, France, n° 106, September, 1967.

2. Russel, H. W., "Principle of Heat Flow in Porous Insulators," Journal of the American Ceramic Society, vol. 18, no. 1, pp. 1-5, 1935.

3. Loeb, A. L., "Thermal Conductivity: VIII, A Theory of Thermal Conductivity of Porous Materials," Journal of the American Ceramic Society, vol. 37, no. 2, pp. 96-99, 1954.

4. Woodside, W., "Calculation of the Thermal Conductivity of Porous Media," Canadian Journal of Physics, vol. 36, pp. 815-823, 1958.

5. Godbee, H. W. and Ziegler, W. T., "Thermal Conductivities of MgO, Al_2O_3, and ZrO_2 Powders to 850°C. II. Theoretical, "Journal of Applied Physics, vol. 37, no. 1, pp. 56-65, January, 1966.

6. Luikou, A. V., Shashkou, A. G., Basilieu, L. L., and Fraiman, Yu. E., "Thermal Conductivity of Porous Systems," International Journal of Heat and Mass Transfer, vol. 11, pp. 117-140, 1968.

7. Krupiczka, R., "Analysis of Thermal Conductivity in Granular Materials," International Chemical Engineering, vol. 7, no. 1, pp. 122-144, January, 1967.

8. Maxwell, J. C., A Treatise on Electricity and Magnetism, 3rd ed., vol. I, Chapter 9, Article 314, Dover, New York, 1954.

9. Rayleigh, "On the Influence on Obstacles in Rectangular Order Upon a Medium," Philosophical Magazine, vol. 34, pp. 481-502, 1982.

10. Fricke, H., "A Mathematical Treatment of the Electric Conductivity and Capacity of Disperse Systems," The Physical Review, vol. 24, pp. 575-587, November, 1924.

11. Batchelor, G. K. and O'Brien, R. W. , "Thermal or Electrical Conduction Through a Granular Material," Proceedings of the Royal society of London, Series A, vol. 355, no. 1682, pp. 313-333, July, 1977.

12. Woodside, W. and Messmer, J. H., "Thermal Conductivity of Porous Media. I. Unconsolidated Sands," Journal of Applied Physics, vol. 27, no. 32, no. 9, pp. 1688-1699, September, 1961.

13. Lichteneker, V. K., "Die Dielektrizitätskonstante natürlicher and Künstlicher Mischköorper," Physikalische Zeitschrift, vol. 27, no. 415, pp. 115-158, March, 1926.

14. Frand, J. and Kingtery, W. D., "Thermal Conductivity IX, Experimental Investigation of Effect of Porosity on Thermal Conductivity," Journal of the American Ceramic Society, vol. 37, no. 2, pp. 99-107, 1954.

15. Jaguaribe, E. F. and Beasley, D. E., "Modeling of the Effective Thermal Conductivity and Diffusivity of a Packed Bed with Stagnant Fluid," International Journal of Heat and Mass Transfer, vol. 27, no. 3, pp. 399-407, 1984.

16. Cheng, S. C. and Vachon, R. I., "A Technique for Predicting the Thermal Conductivity of Suspensions, Emulsions, and Porous Materials," International Journal of Heat and Mass Transfer, vol. 13, pp. 537-546, 1970.

17. Ofuchi, K. and Kunii, D., "Heat Transfer Characteristics of Packed Beds with Stagnant Fluids," International Journal of Heat and Mass Transfer, vol. 8, pp. 749-757, 1965.

General References

1. Chapra, Steven C. and Canale, Raymond P., Numerical Methods for Engineers. 2nd ed. McGraw-Hill, 1988.

2. Niederreiter, Harold, Random Number Generation and Quasi-Monte Carlo Methods. Philadelphia: Society for Industrial and Applied Mathematics, 1992.

3. Somerton, Craig W., "A Numerical Model for the Effective Thermal Conductivity of a Porous Medium." (Unpublished paper.)